Investigation into the Photoluminescence Red Shift in Cesium Lead Bromide Nanocrystal Superlattices

Dmitry Baranov,[a*] Stefano Toso,[a] Muhammad Imran,[a,b] Liberato Manna[a*]

[a]Nanochemistry Department, Istituto Italiano di Tecnologia, Via Morego 30, 16163 Genova, Italy

[b]Dipartimento di Chimica e Chimica Industriale, Università degli Studi di Genova, Via Dodecaneso 31, 16146 Genova, Italy

*E-mail: dmitry.baranov@iit.it, liberato.manna@iit.it

Contents:

S1. Photoluminescence (PL) red shift in a solid of $CsPbBr_3$ nanocrystal superlattices (NC SLs)

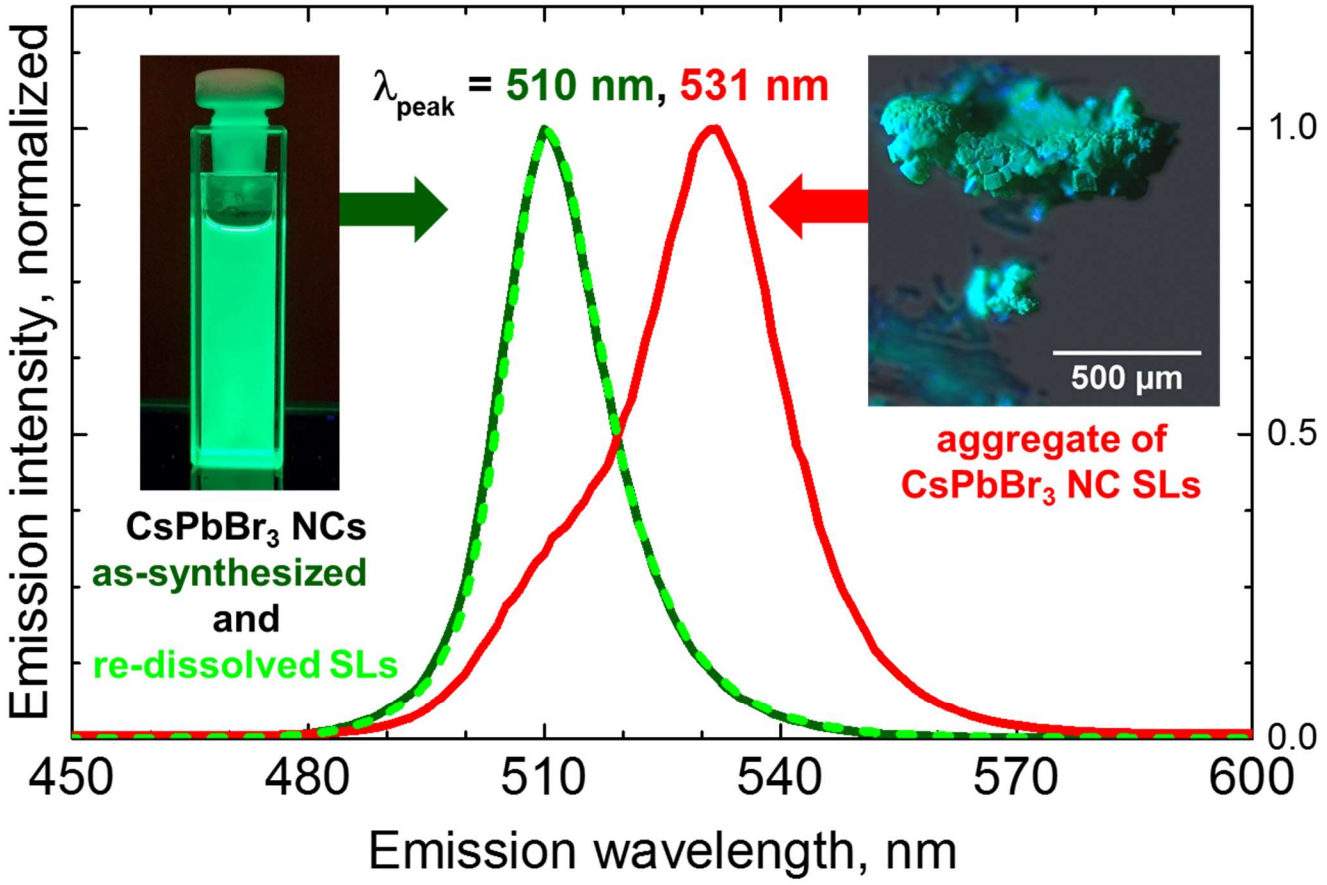

Figure S1. Photoluminescence spectra from a diluted solution of as-synthesized $CsPbBr_3$ NCs in toluene (solid green curve), a millimeter-sized aggregate of NC SLs (solid red curve), and the very same SLs re-dissolved in toluene (dashed bright green curve). The spectra were recorded with λ_{exc} = 350 nm in 90° geometry. The PL red shift is ~21 nm (~96 meV).

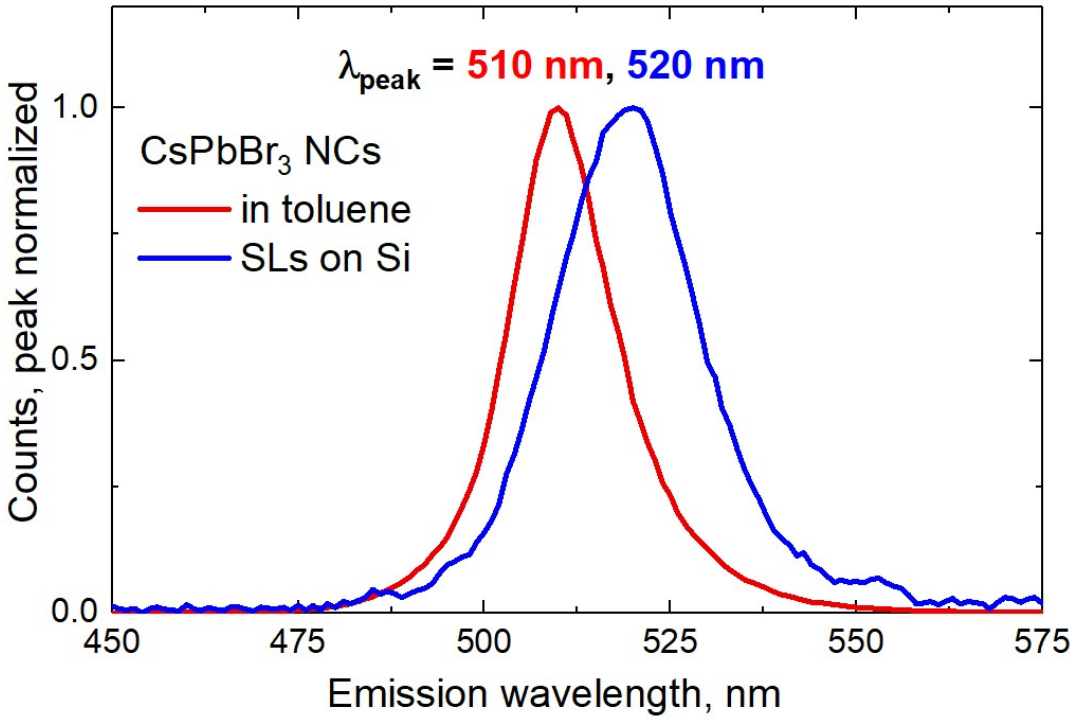

Figure S2. Photoluminescence spectra from a diluted solution of $CsPbBr_3$ NCs in toluene (red curve) and a solid of $CsPbBr_3$ NC SLs deposited on top of a Si wafer (blue curve, ~5x2 mm illumination area). Excitation wavelength 350 nm, spectra recorded at 90° geometry. The PL red shift for this sample ~10 nm (~47 meV). A smaller red shift compared to the sample shown in Figure S1 is rationalized as arising from the different amount of SLs on the wafer and possibly a different fraction of SLs with defects in the sample.

S2. Experimental details

a) Chemicals.

Lead (II) bromide ($PbBr_2$, ≥98%, 211141-100G), cesium carbonate (Cs_2CO_3, 99%, 441902-100G), 1-octadecene (technical grade, 90%), oleylamine (≥98% primary amine, HT-OA100-1.5KG), oleic acid (technical grade, 90%), toluene (anhydrous), hexane (anhydrous), and perfluorodecalin (95%, P9900-25G) were purchased from Sigma Aldrich and used as received without further purification. Lead (II) bromide was opened, stored, and handled inside a nitrogen-filled glovebox. Volumes of liquid reagents were measured using either disposable syringes or mechanical micropipettes.

b) Synthesis of $CsPbBr_3$ NCs

The stock solution of cesium oleate precursor was prepared by reacting 400 mg of cesium carbonate with 1.75 ml of oleic acid in 15 ml of octadecene inside a 40 ml glass vial heated to 100-120 ºC (the temperature of the mixture) under the flow of nitrogen; the reaction was considered complete once all visible solid disappeared. The precursor was cooled down to room temperature under stirring, turning cloudy white. That room temperature cloudy suspension was used for subsequent injections without pre-heating.

Next, 72±2 mg of $PbBr_2$ were combined in a 20 ml glass vial with 5 ml of octadecene-1, 0.5 ml of oleylamine and 0.05 ml of oleic acid. The vial was equipped with a magnetic stirring bar, a cap with a septum, a thermocouple, and placed into an aluminum block preheated to ~200 ºC on top of a hotplate/magnetic stirrer. The block had a machined cylindrical cavity to snugly fit the lower ~2 cm of the vial, providing quick heating of the reaction mixture. The stirring was switched on immediately after the vial was placed in the block. As soon as the temperature of the reaction mixture reached ~170-175 ºC and all $PbBr_2$ was dissolved (as judged visually), the vial was transferred outside of the block and fixed with a clamp above a non-heated magnetic stirrer, and the stirring was turned back on. At that point, the reaction mixture starts to cool down in the air. As soon as the temperature reached ~165 ºC, 0.5 ml of the

cesium oleate precursor were swiftly injected. Upon injection, the clear and colorless reaction mixture immediately turned into a clear yellow one, which became cloudy bright green upon cooling. The cooling was accomplished by leaving reaction mixture under stirring in still air.

c) Isolation of $CsPbBr_3$ NCs and preparation of the stock solution for self-assembly

Once the reaction mixture cooled down to within ~10 degrees of the room temperature, it was split equally into four 4 ml vials using a Pasteur pipette. The vials were centrifuged for 3 minutes at 4000 rpm, yielding bright green-yellow precipitate at the bottom and a clear bright green-yellow supernatant. The supernatant was discarded. The vials were centrifuged again (1 min at 4000 rpm) to collect the non-decanted fraction of the liquid and to further clean the precipitate from the residual supernatant. For that centrifugation step the vials were oriented in the centrifuge such that the precipitate was pointing outwards, so the remaining liquid could be collected in the lower and opposite part of the vial. After the centrifugation, the liquid was removed with a cotton tip, and the centrifugation/cotton tip step repeated once more. Next, the solid (in one of four vials) was dissolved in 1 ml of anhydrous toluene and PL, and absorbance spectra of the NC batch were measured in a quartz cell by diluting 5-10 μL of the NC solution in 1000 μL of toluene. The NC batches were deemed suitable for self-assembly experiments when full width at half maximum (FWHM) of the emission spectra was <80 meV. No effort was made to further narrow the PL FWHM by changing the reaction conditions, nor by size-selective precipitation with anti-solvents. Absorbance was measured through 10 mm pathlength, and the NC concentration was calculated from Beer's law by using optical density at 335 nm in and a published size-dependent extinction coefficient.[1] Typical concentrations obtained in this way of sample preparation varied in the range of ~0.3-1 μM, depending on the batch of NCs. To make a stock solution for self-assembly experiments, the content of another vial was dissolved in 0.5-2 ml of anhydrous hexane to obtain a solution with a concentration of ~0.8-1 μM and filtered through 0.45 μm hydrophobic PTFE syringe filter. The hexane solution of NCs was prepared and used shortly before self-assembly.

d) Self-assembly at the surface of perfluorodecalin (PFD)

The self-assembly setup was constructed in the following way. A transparent Eppendorf-type 3 ml plastic vial with a cap removed was placed in a 20 ml glass vial, and 500 μL of clear and colorless PFD were added to it. Next, a 3 cm piece of an opaque PTFE tubing [20533 Supelco, tubing L × O.D. × I.D. 25 ft × 1/4 in. (6.35 mm) × 0.228 in. (5.8 mm)] cleaned from the dust particles with compressed air was inserted inside the Eppendorf vial forming a hydro- and lipophobic well to host the formation of NC SLs. 10-100 μL of NC solution in hexane were carefully placed on top of the PFD inside the PTFE tube using a micropipette. The 20 ml glass vial was closed with a screw cap without causing much agitation, placed on a still surface and covered with aluminum foil to protect from ambient lights. The hexane diffusion into PFD is visually manifested by a gradual decrease in the volume of the NC solution. For 50 μL of NC solution, the process takes ~5 hrs; the exact duration varies depending on the total volume of NC solution and ambient temperature. Once the hexane diffusion is complete, a green and brightly luminescent solid of NC SLs remains on top of the PFD surface loosely attached to the walls of the PTFE tube (Figure 1c in the main text, Figure S4).

e) Handling of SLs

Upon completion of the hexane diffusion and prior to manipulations with the SLs, the PTFE tube was carefully taken out from the Eppendorf vial. During that step, most of the NC SLs detach from the walls of the PTFE tube, fall into the PFD liquid and stick to the walls of the Eppendorf tube. From here, the SLs were handled in two ways: as a suspension in oleic acid or deposited onto solid substrates directly from PFD with the help of ultrasonication.

To disperse the SLs in oleic acid, the perfluorodecalin was decanted, leaving the solid of NC SLs stuck to the walls of the Eppendorf vial. The solid was dried under a gentle flow of nitrogen, and a small volume (50-100 μL) of neat oleic acid was added, following by shaking with hand or on a vortex mixer. The latter resulted in the formation of a luminescent suspension (Figure 1c in the main text, right photo). The

suspension of SLs in oleic acid is not stable over time (SLs of $CsPbBr_3$ NC partially dissolve or deform while turning yellow within 24 hours).

To directly deposit SLs onto a glass or a silicon substrate the PFD was not decanted. A rectangular piece of the substrate was immersed in the vial containing PFD and a solid of SLs, the vial was capped and partially immersed into the water-filled sonicator bath for ~1-15 seconds under sonication. The sonication causes SLs to simultaneously disperse inside the PFD and stick to the substrate. The sonication-assisted transfer of SLs is demonstrated in Supporting Video 1. The effect of the sonication power onto the transfer of SLs has not been investigated.

f) Characterization of NCs

Average size and size distribution of the synthesized NCs were characterized using transmission electron microscopy (TEM) on a JEM 1400-Plus JEOL microscope operating at an acceleration voltage of 120 kV. One drop of the sample solution was deposited onto carbon-coated copper grids using a Pasteur pipette, and the solvent was let to evaporate.

The phase purity of NCs was inspected by X-ray diffraction (XRD) measurements. XRD was performed on a PANalytical Empyrean X-ray diffractometer using a Cu Kα cathode (λ=1.5406 Å) operating at 45 kV and 40 mA. The samples for XRD were prepared by drop-casting concentrated NC solutions from hexane or toluene solutions onto a zero diffraction silicon wafer and letting the solvent evaporate. The recorded diffraction patterns matched best with the pattern of orthorhombic $CsPbBr_3$, [COD (Crystallography Open Database) card no. 4510745,[2] reference code 96-451-0746 in High Score ver. 4.7], consistent with prior reports.[3, 4]

Absorbance and PL spectra of diluted $CsPbBr_3$ NC solutions in toluene or hexane were recorded using Cary 500 spectrophotometer and Cary Eclipse spectrofluorimeter, respectively. The spectra were measured in 10x4 mm quartz cuvettes (Hellma Analytics, 114F) on freshly diluted samples. A wavelength of 350 nm (2.5-5 nm excitation and emission slit widths) was used for excitation. To report the emission

peak and FWHM in eV, the PL spectra were converted from the wavelength to energy scale using appropriate fundamental constants and by multiplying each intensity by $\lambda^{2.5}$.

g) Characterization of NC SLs

Optical microscopy of SL suspensions in oleic acid was performed using Nikon 80i or Leica DM2500M optical microscopes equipped with digital cameras. The samples were prepared by placing a small drop (~3-5 μl) of freshly prepared SL suspension in oleic acid on top of a rectangular microscope slide and covering it with a thin glass coverslip. High resolution scanning electron microscopy (HRSEM) and energy dispersive X-ray spectroscopy (EDS) of NC SLs were performed on a sample of SLs deposited on top of a ~5x15 mm piece of a Si wafer with the help of ultrasonication. Optical profilometry experiments were performed using ZETA-20 true color 3D optical profiler equipped with a digital camera for image recording under white light illumination. The samples were prepared by ultrasound-assisted deposition of NC SLs onto glass or silicon substrates. See Supporting Video 1 for a demonstration of the ultrasonication-assisted transfer of SLs.

Confocal PL microscopy on SLs grown on the PFD surface and control samples (NC dispersion in ODE and an NC film) was performed using a Nikon A1 confocal laser microscope and utilizing two excitation sources: 488 nm (air-cooled Ar-ion laser, Melles Griot, 35-IMA-840-019) or 401 nm (solid state laser, Coherent, 1170506). The laser power setting was kept at 0.5-1%, and the resolution of a 32-channel spectral detector set at 2.5 nm during the experiments. The samples were prepared in a similar way as for the optical microscopy measurements except the glass coverslip was fixed to the microscope glass slide by a blue nail lacquer (KIKO Make Up Milano). Objectives used for the experiments were either Plan Apo 20x DIC M N2 or the oil immersive objective Plan Apo VC 60x Oil DIC N2. The spectrally-resolved imaging data (as *.nd2 files) were acquired using Nikon NIS-Elements High Content Analysis ver. 4.30.02 and viewed in Nikon NIS-Elements Viewer ver. 4.20.00.

Confocal PL microscopy of $CsPbBr_3$ NC SLs grown by a slow solvent evaporation on the tilted Si wafer was performed using Leica TCS SP5 Confocal microscope [Leica Microsystems, Wetzlar, Germany; equipped with a supercontinuum laser excitation source, acousto-optical beam splitter (AOBS®) for separation of excitation and emission wavelengths and Leica HyD SP detector]; 10X air objective lens was used (Leica HCX PL APO CS 10.0x0.40 DRY UV), the excitation wavelength was set to 488 nm at 3% relative laser power. The spectrally-resolved images were recorded with the emission detection bandwidth of 5 nm and 3-3.1 nm spectral resolution over 490-580 nm wavelength range.

The spectrally-resolved imaging data (except *z* series) were opened and processed as stacks using an open source Fiji distribution of ImageJ ver. 1.52e.[6-8] The spectral profiles of individual SLs and areas of interest were obtained by drawing polygonal regions of interest (ROIs) around selected SLs and performing "Plot Z-stack Profile" operation in Fiji, which yielded a plot of the brightness of ROI (mean grey value, proportional to the number of emitted photons) as a function of the slice number (emission wavelength bin with the width of the spectral resolution). The colored images shown in Figure 3 of the main text were obtained by using "Temporal Color Code" hyperstacks function in Fiji with LUT setting "Spectrum." The spectrally-resolved data containing *z* slices were viewed and processed using Nikon NIS-Elements Viewer ver. 4.20.00.

S3. Average size of $CsPbBr_3$ NCs

The size distribution was obtained from TEM images using freely available ImageJ software and applying a thresholding analysis.[9, 10] The images were processed with the "FFT Bandpass Filter" setting 1.5-40 nm range for small-large structures, the "Brightness/Contrast" was adjusted automatically, and the "default" threshold applied. After examining the results of thresholding, the range of measured areas was set to 15-96 nm^2 in the "Analyze Particles…" menu to cut off artificially small or large structures from the analysis.

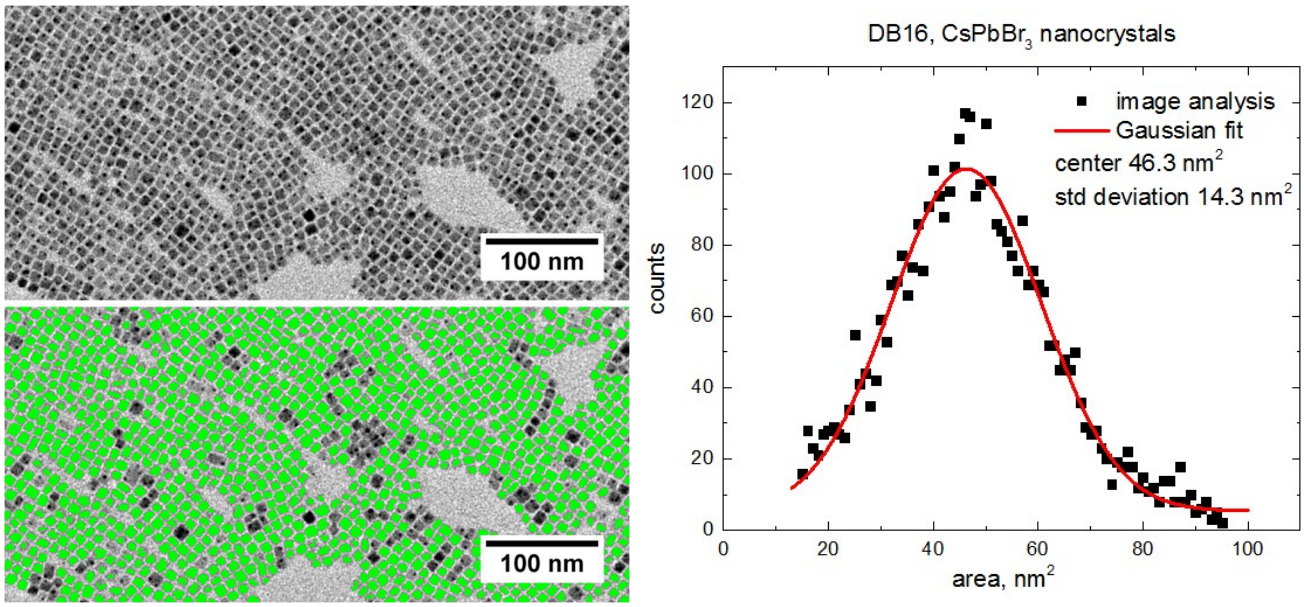

Figure S3. (top left panel) a fragment of TEM image, (bottom left) overlaid green masks of the measured nanocrystals after the image processing with the thresholding analysis, (right) area distribution obtained from processing several TEM images yielding a total of 3890 measured nanocrystals and the corresponding Gaussian fit. The average area is 46.3±14.3 nm^2, which translates to ~6.8±1 nm edge length assuming the square shape of $CsPbBr_3$ nanocrystals projections.

S4. Photographs of the self-assembly setup

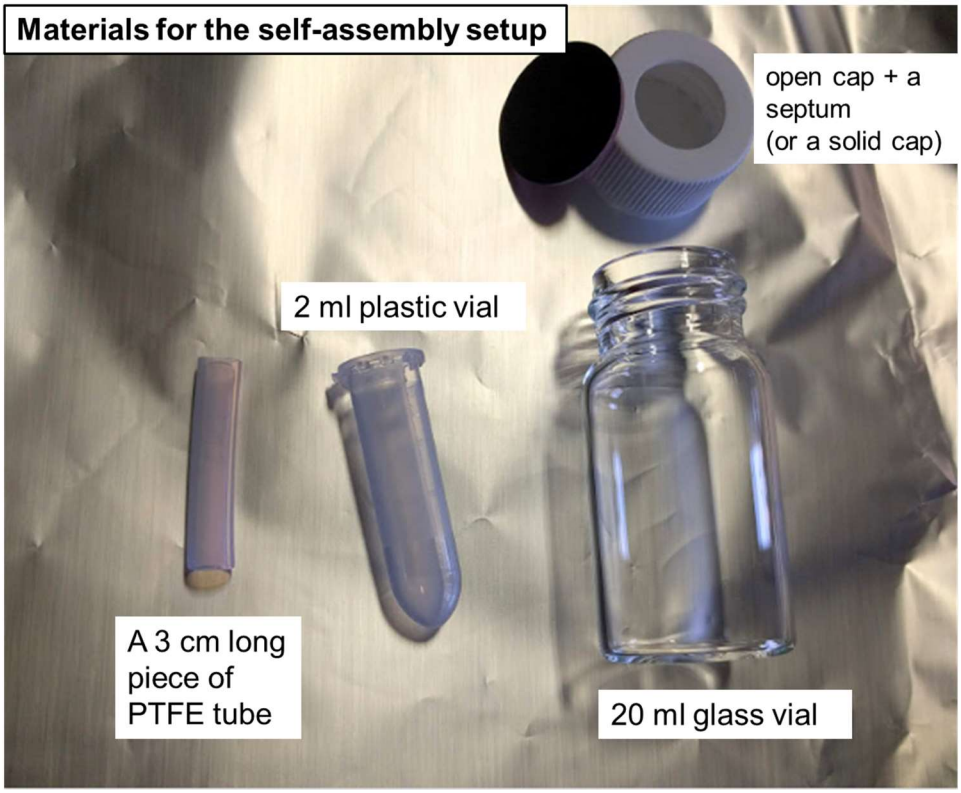

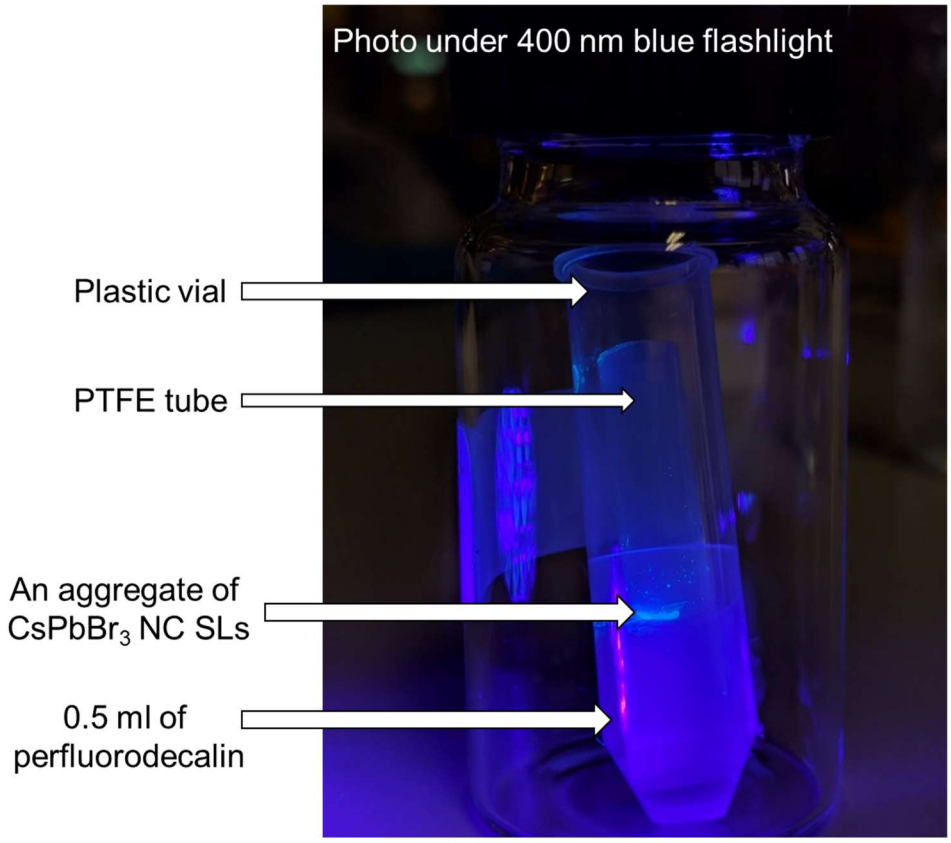

Figure S4. Photo of the self-assembly setup at the beginning and end of the process.

S5. Optical microscopy images of the $CsPbBr_3$ NC SL solid isolated after the self-assembly

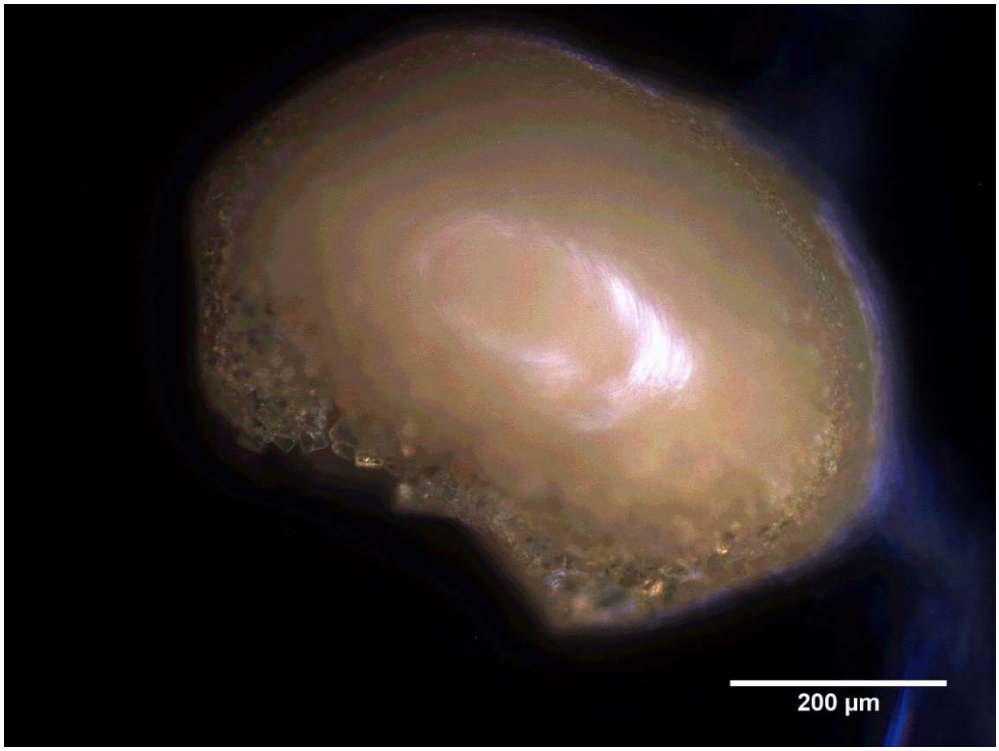

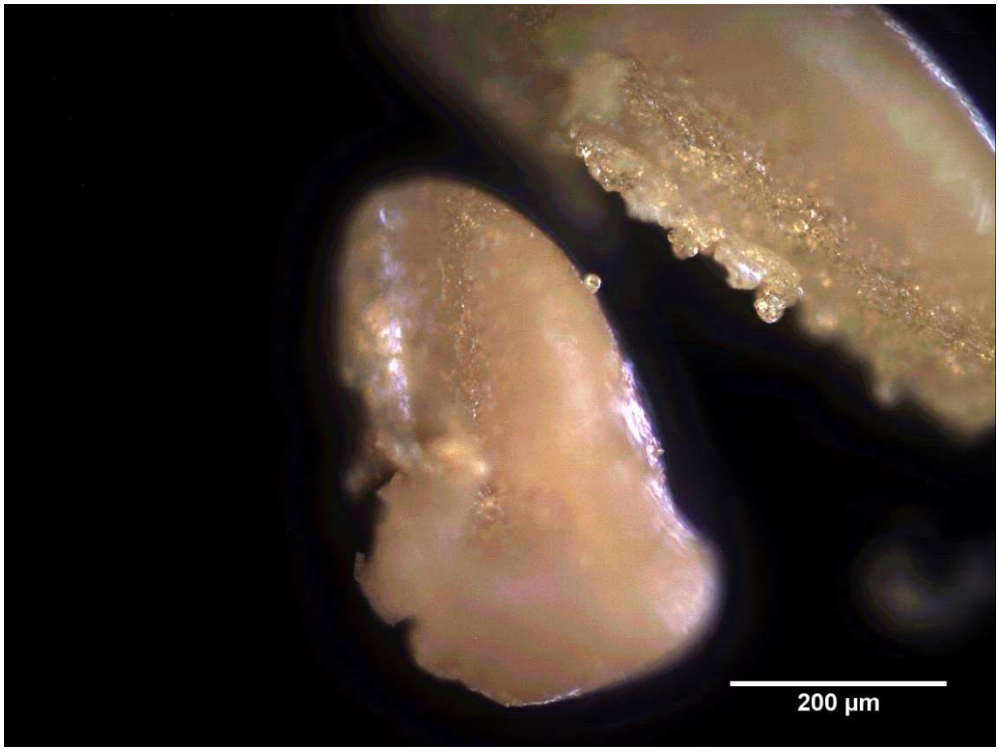

Figure S5. Optical microscopy images of a solid consisting of $CsPbBr_3$ NC SLs (~1-10 µm in size) collected from the surface of PFD after hexane diffusion. The images were taken with Leica DM2500 M optical microscope.

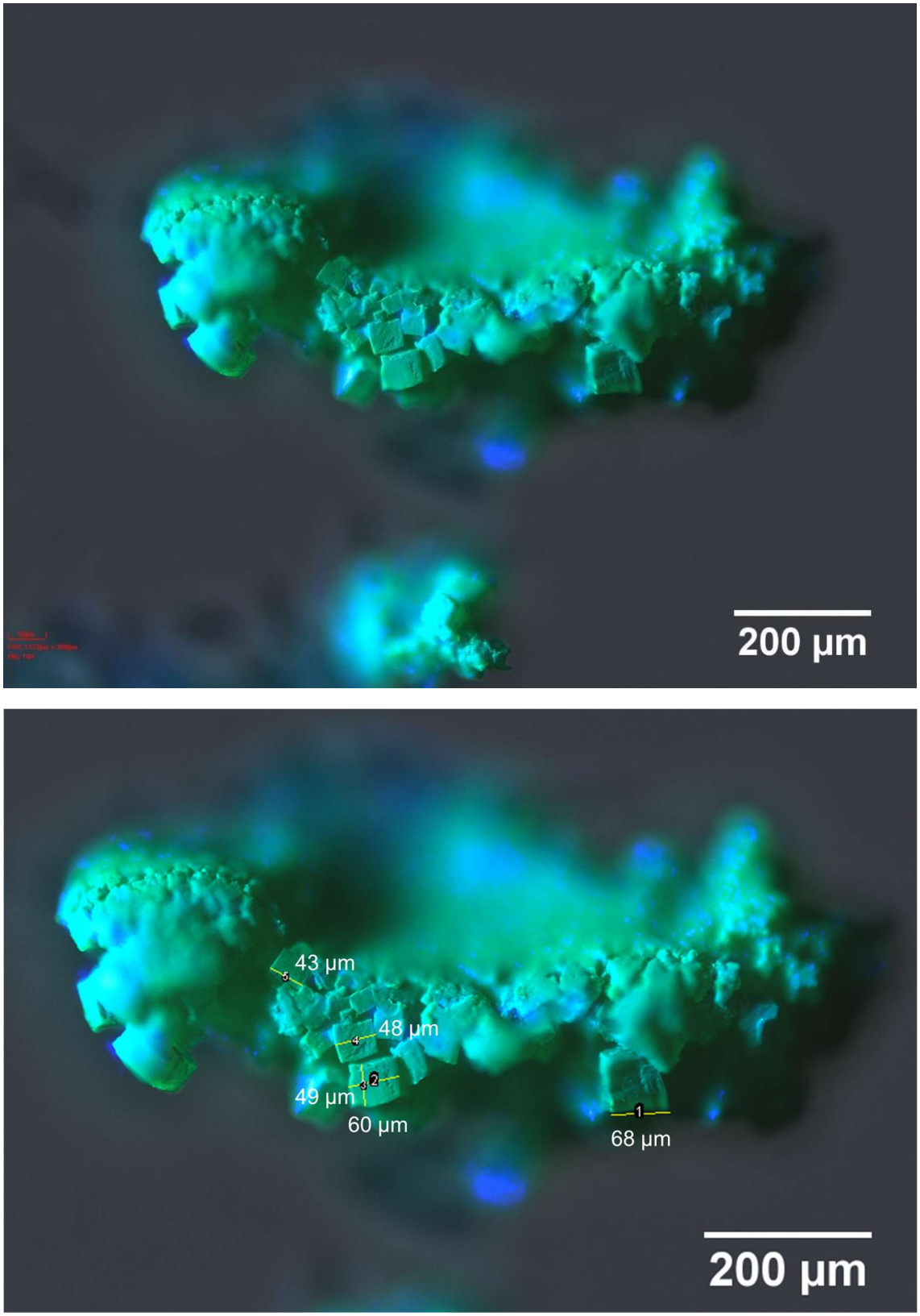

Figure S6. Optical microscopy images of a solid consisting of $CsPbBr_3$ NC SLs (up to ~70 µm in size) and collected from the surface of PFD after hexane diffusion. The images were taken with ZETA-20 optical profiler under 400 nm illumination with a UV LED flashlight.

S6. Optical microscopy images of $CsPbBr_3$ NC SLs suspended in oleic acid

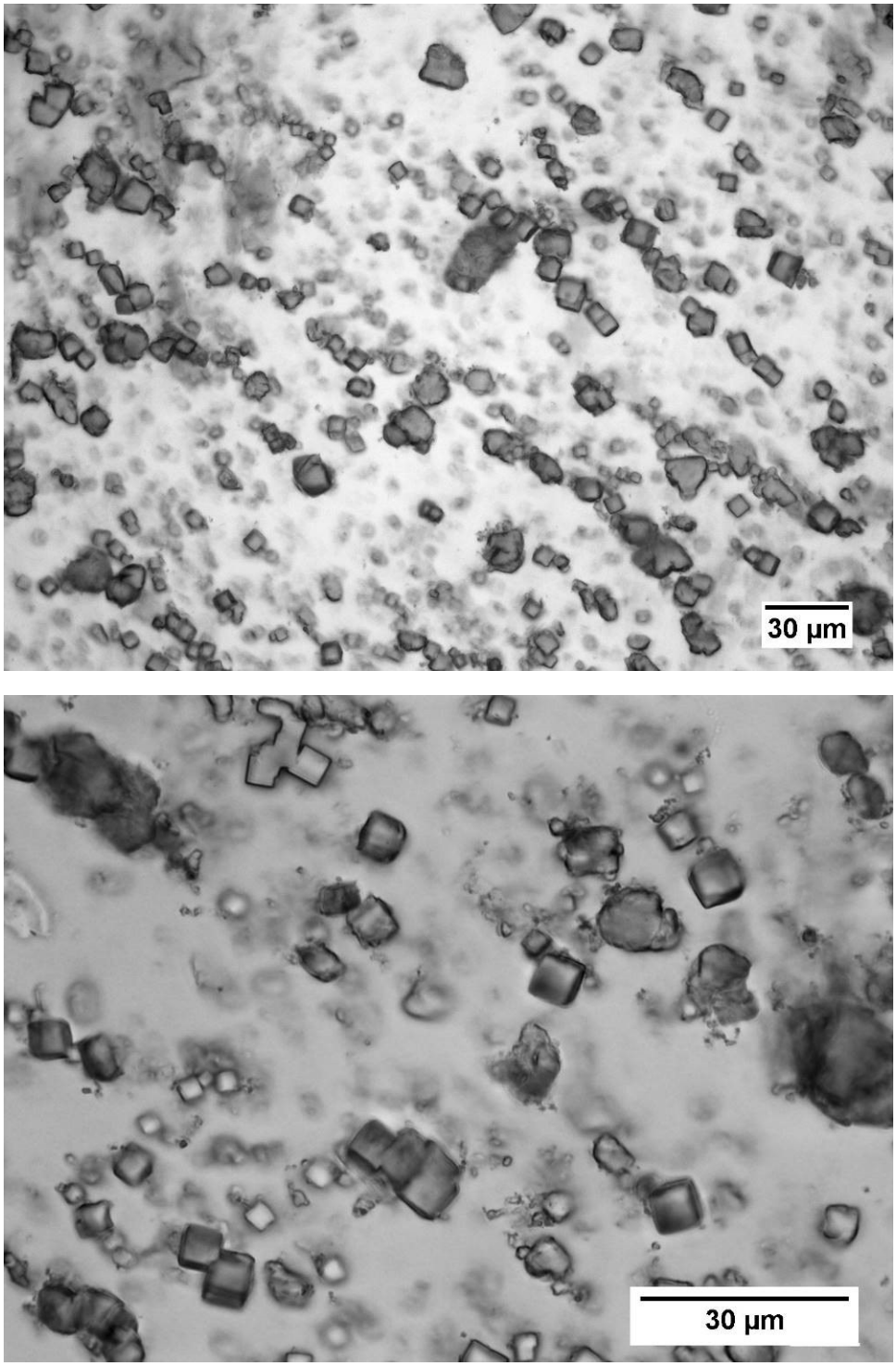

Figure S7. Optical microscopy images of $CsPbBr_3$ NC SL suspension in oleic acid obtained from dispersing the NC SL solid. The images were acquired with a Nikon 80i microscope.

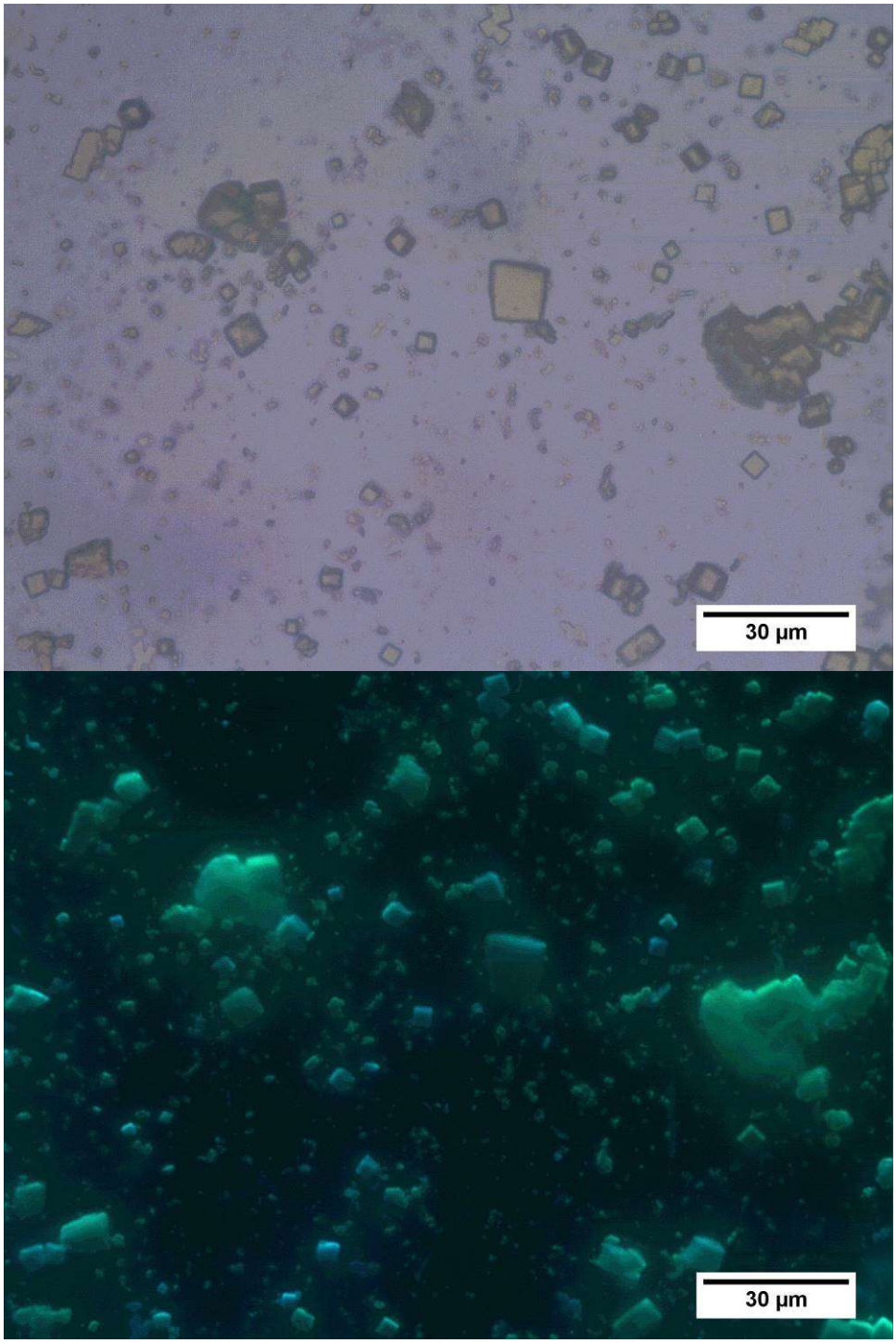

Figure S8. Optical microscopy images of $CsPbBr_3$ NC SL suspension in oleic. The images were acquired with Leica DM2500 M optical microscope under white light (top image), and 400 nm UV LED flashlight (bottom image) illumination.

S7. Optical profilometry of $CsPbBr_3$ NC SLs on the glass and silicon substrates

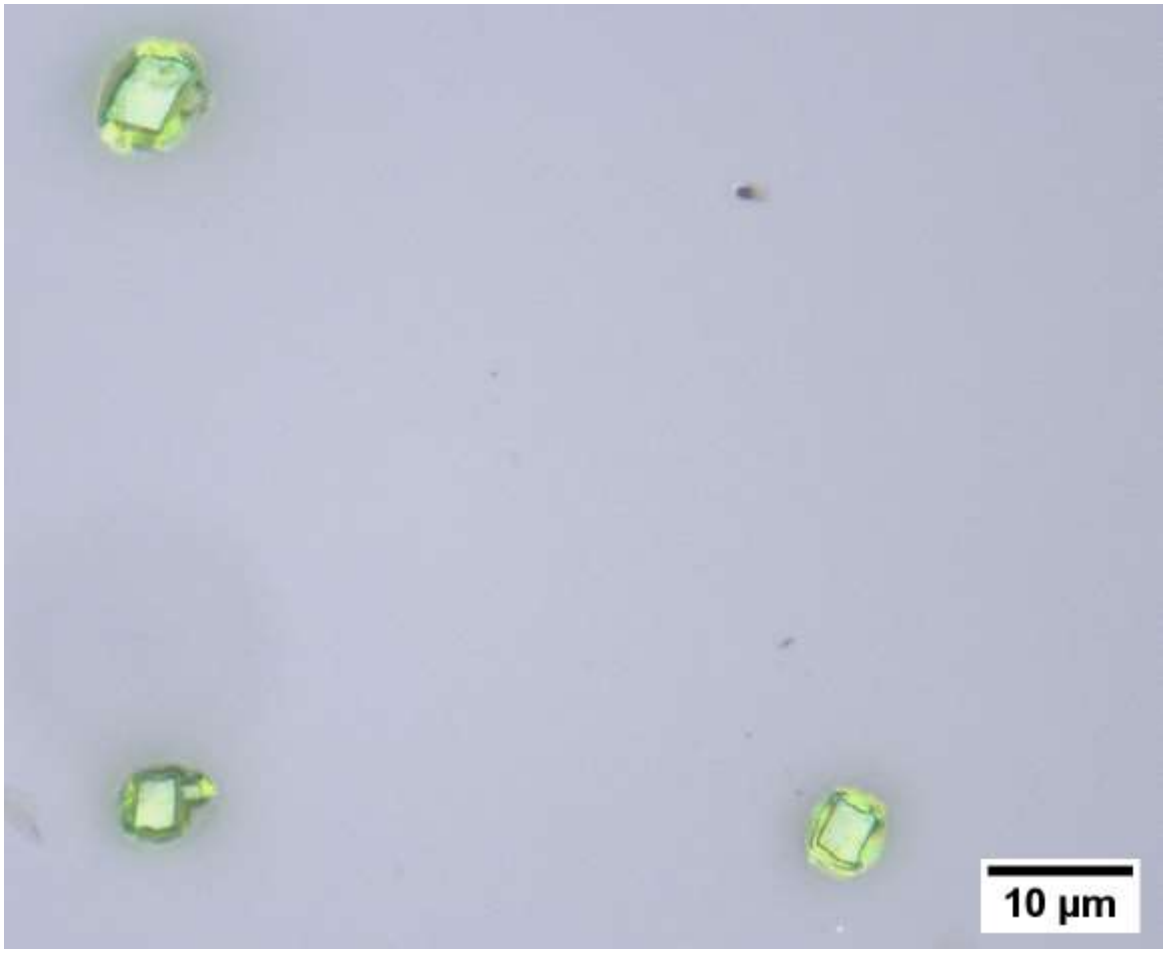

Figure S9. Optical profilometry image of three small $CsPbBr_3$ NC SLs (~3-6 µm dimensions) deposited on a glass slide by sonication. The image was acquired with ZETA-20 optical profiler.

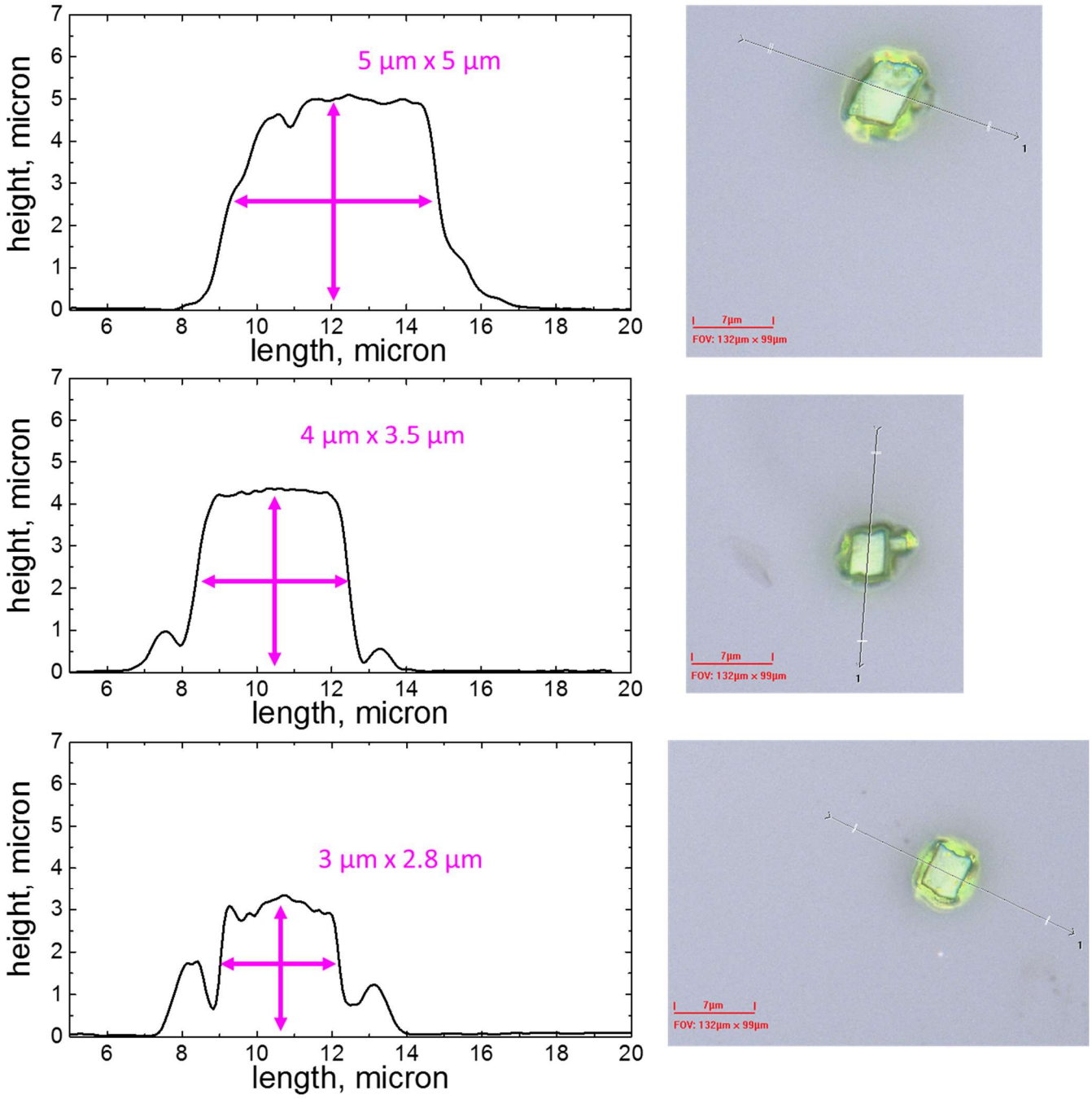

Figure S10. Line slices through the 3D profiles of $CsPbBr_3$ NC SLs shown in Figure S7 above, demonstrating their nearly isotropic shapes of the SLs. The data were acquired with ZETA-20 optical profiler. The side wings in the middle and bottom plots are either optical artifacts or residual organics.

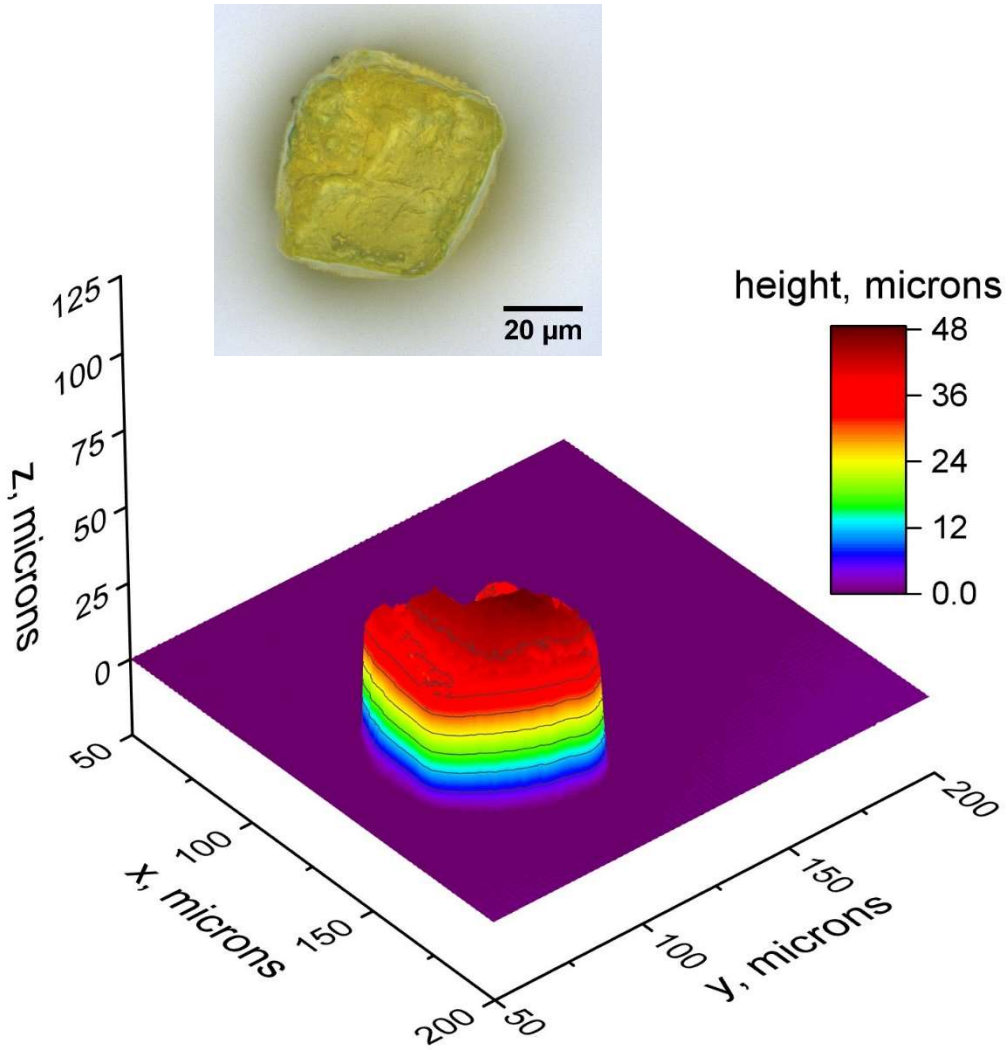

Figure S11. A topological profile of one of the large $CsPbBr_3$ NC SLs and a corresponding optical microscopy image. The data were acquired with ZETA-20 optical profiler.

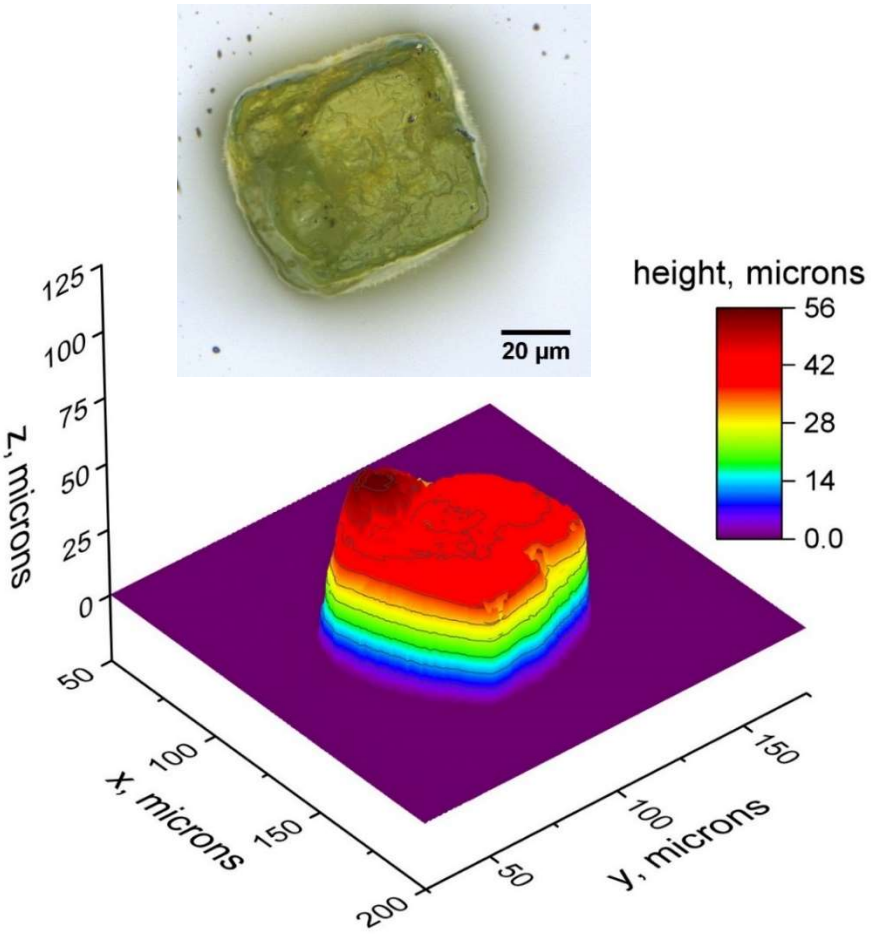

Figure S12. A topological profile of another large $CsPbBr_3$ NC SLs and a corresponding optical microscopy image. The data were acquired with ZETA-20 optical profiler.

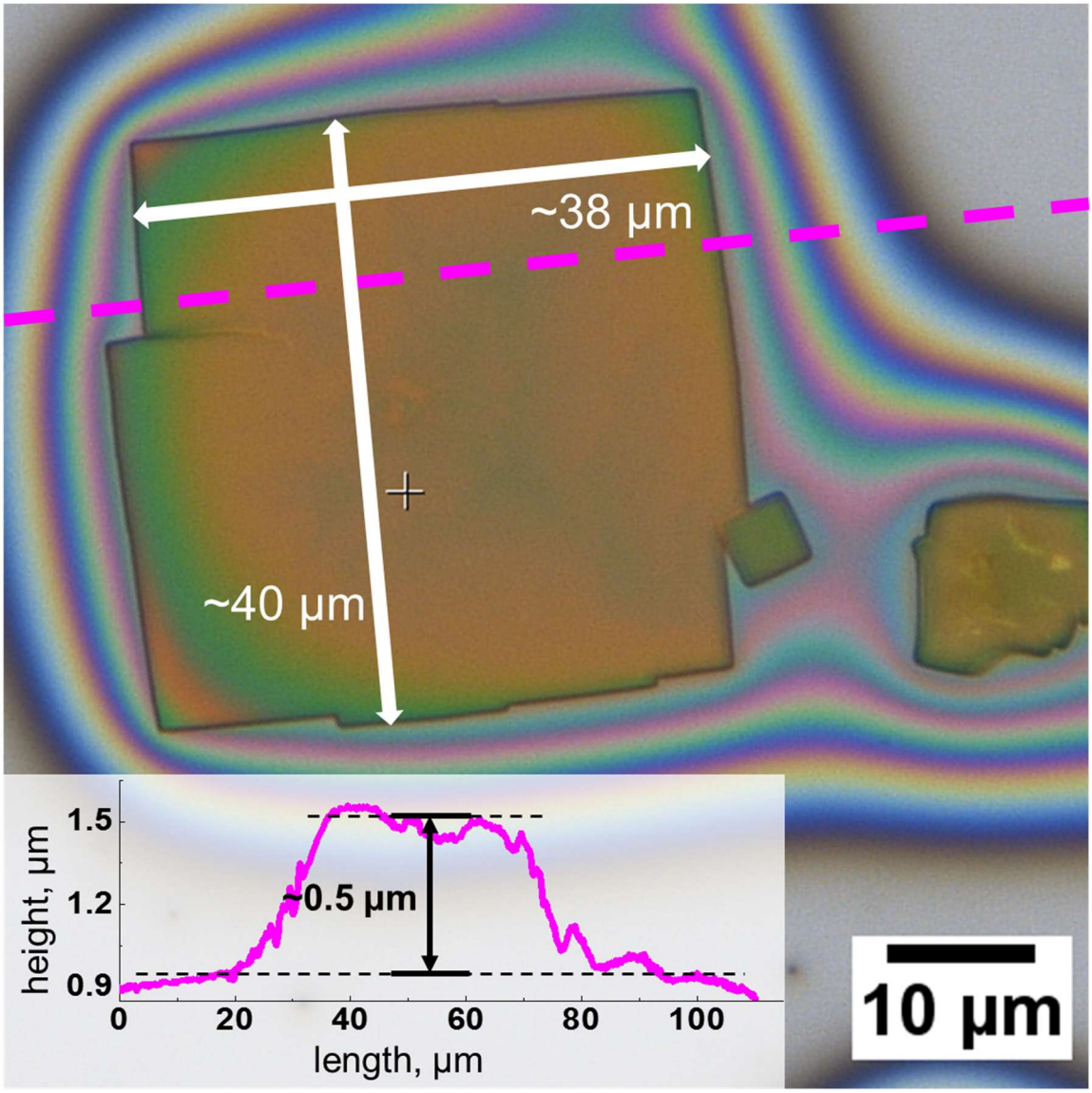

Figure S13. Optical microscopy image and a height characterization of a single ~40 x 40 x 0.5 microns square-like $CsPbBr_3$ NC SL grown by slow solvent evaporation on a tilted Si wafer as described in the main text. A dashed magenta line indicates the location where line profile was taken. The data were acquired with ZETA-20 optical profiler.

S8. Confocal PL microscopy data for $CsPbBr_3$ NC SLs, NC dispersion and NC film.

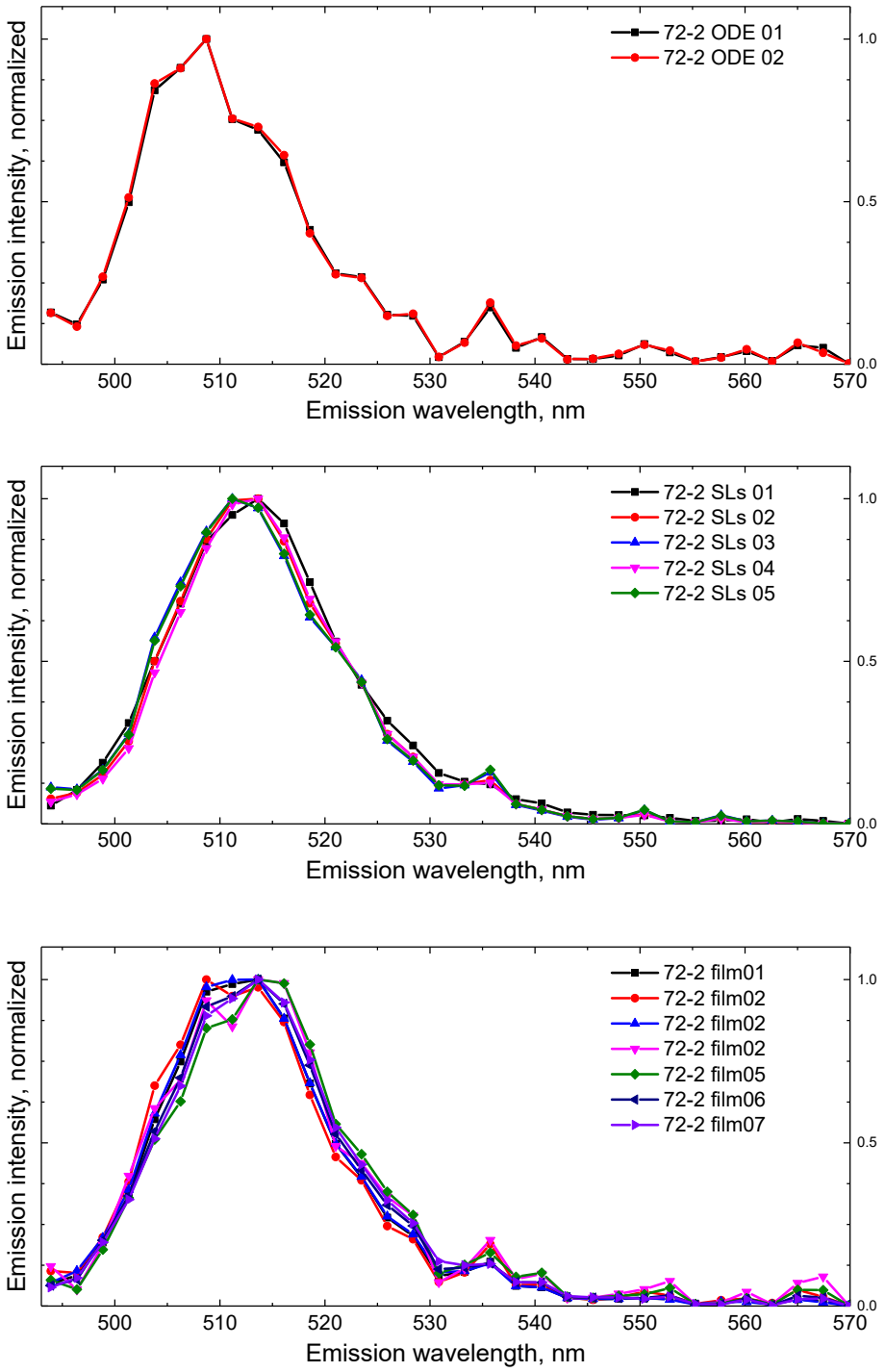

Figure S14. Additional confocal PL microscopy data for three kinds of samples derived from the same $CsPbBr_3$ NCs batch as shown in Figure 2 of the main text: NC dispersion in ODE (top plot), five different clean NC SLs (middle plot), and seven different regions of a drop-casted film (bottom plot).

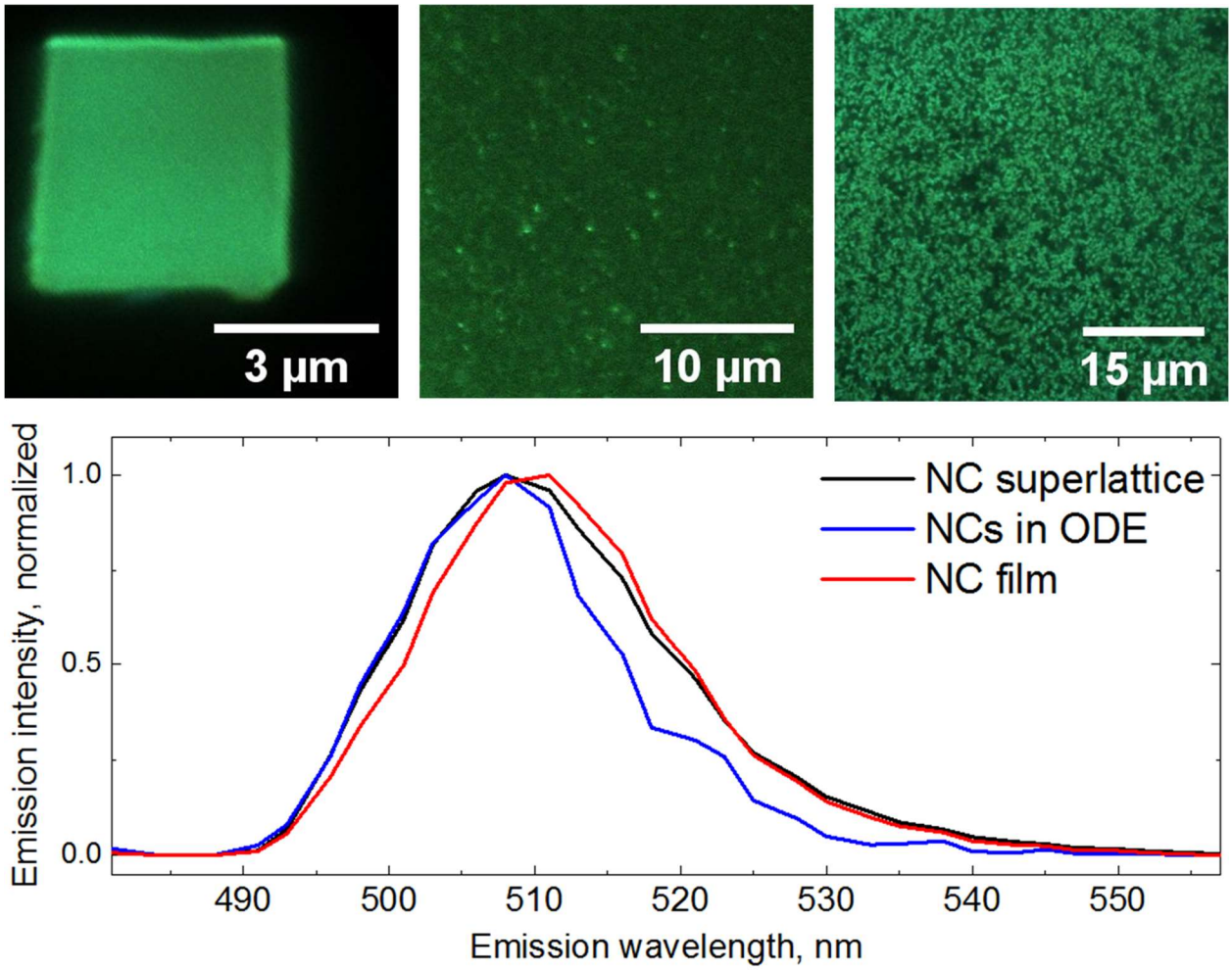

Figure S15. Confocal PL microscopy data for three kinds of samples derived from another batch of $CsPbBr_3$ NCs: individual SL (top left image, black curve spectrum), NC dispersion in octadecene-1 (top middle image, blue curve spectrum), and a film drop-casted from hexane solution (top right image, red curve). The samples were excited with a laser diode, λ_{exc} = 405 nm.

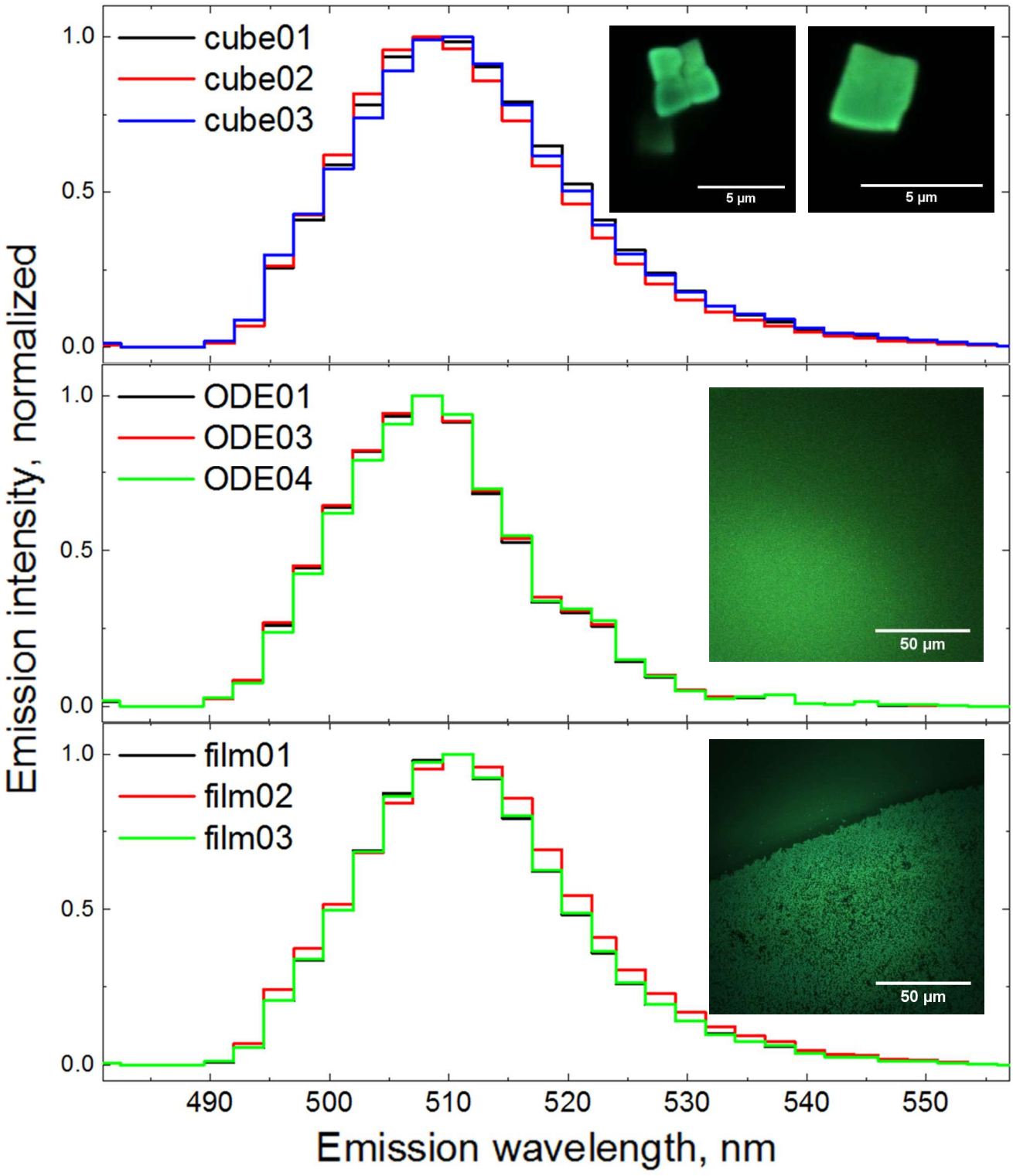

Figure S16. Additional confocal PL microscopy data for the samples shown in Figure S16: three different superlattices (top panel), NC dispersion in ODE (middle), and a drop-casted film (bottom panel).

S9. Confocal PL microscopy *z* slices of a $CsPbBr_3$ NC SL with impurities

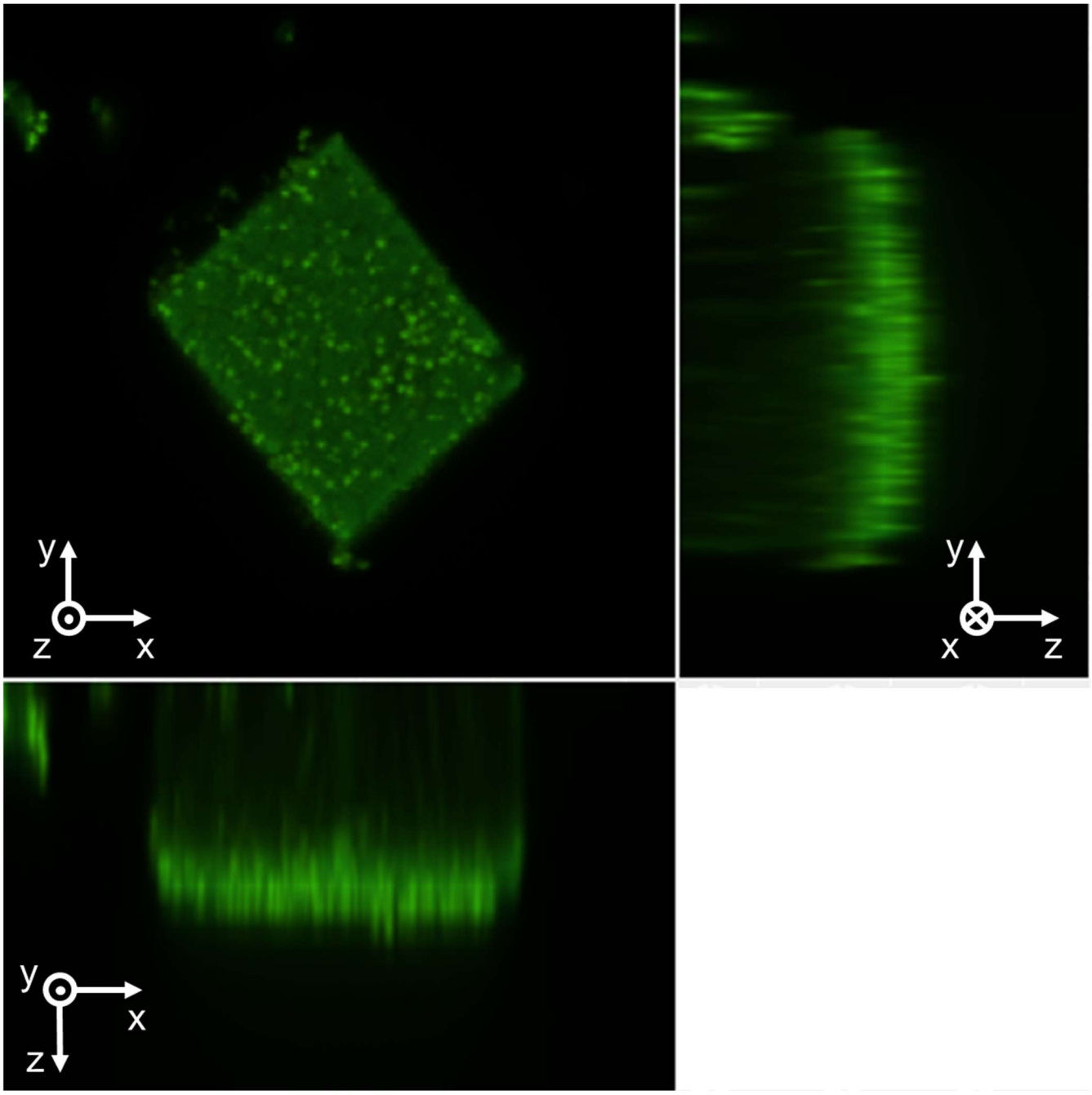

Figure S17. Confocal PL microscopy projections reconstructed from the z slices of the SL with impurities. The impurities appear as bright spots. The projections are shown with all spectral channels on (spectral range of ~481-557 nm). *xy* plane projection (upper left image) has dimensions of 15.55 μm x 15.55 μm, *yz* and *xz* plane projections (upper right and lower left images, respectively) have dimensions of 15.55 μm along *y* and *x*-axes, and 9.00 μm along *z*-axis.

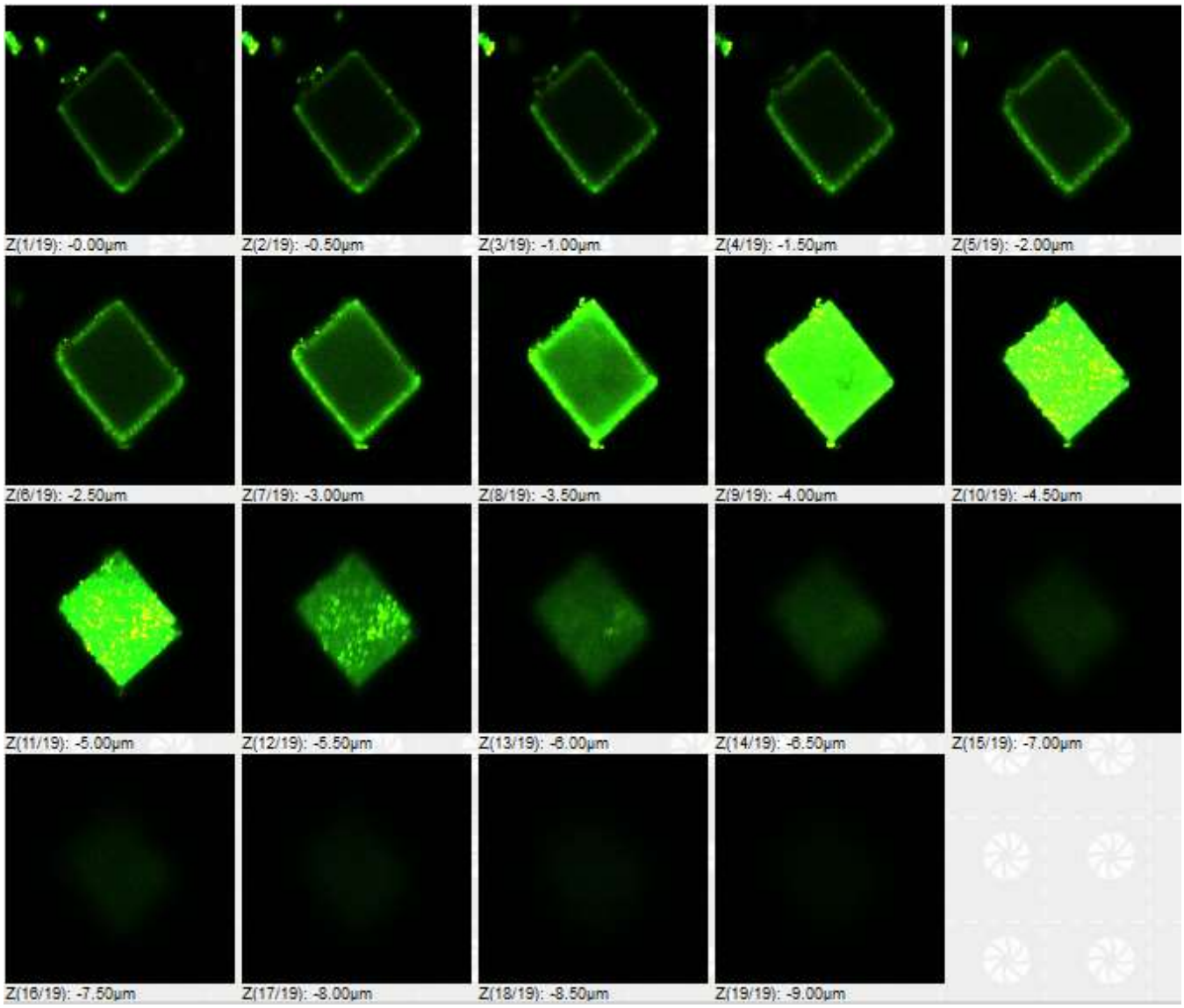

Figure S18. A grid of the z-slices showing the distribution of the PL signal from an SL with impurities as a function of the position of the focal plane. The total of 19 slices are shown, the slices are arranged from left to right in four rows. z step size is 0.5 µm, z range is from "-0.00µm" (bottom of the SL) to "-9.00 µm" (above the top of the SL). Each square has dimensions of 15.55 µm x 15.55 µm (512 x 512 pixels).

z slices 10/19, 11/19, and 12/19 capture the topmost layer of the SL, *z* slices from ~1/19 to 9/19 capture the bulk of the SL. The distribution of the PL signal along *z* dimension visualized in Figure S18 suggests that the bright spots are covering the top surface of the SL, as they are most prominently visible in *z* slices 10/19-12/19. The bright spots are also visible along the perimeter in the *z* slices 1/19-9/19, which further suggests that impurities cover sides of the SL as well.

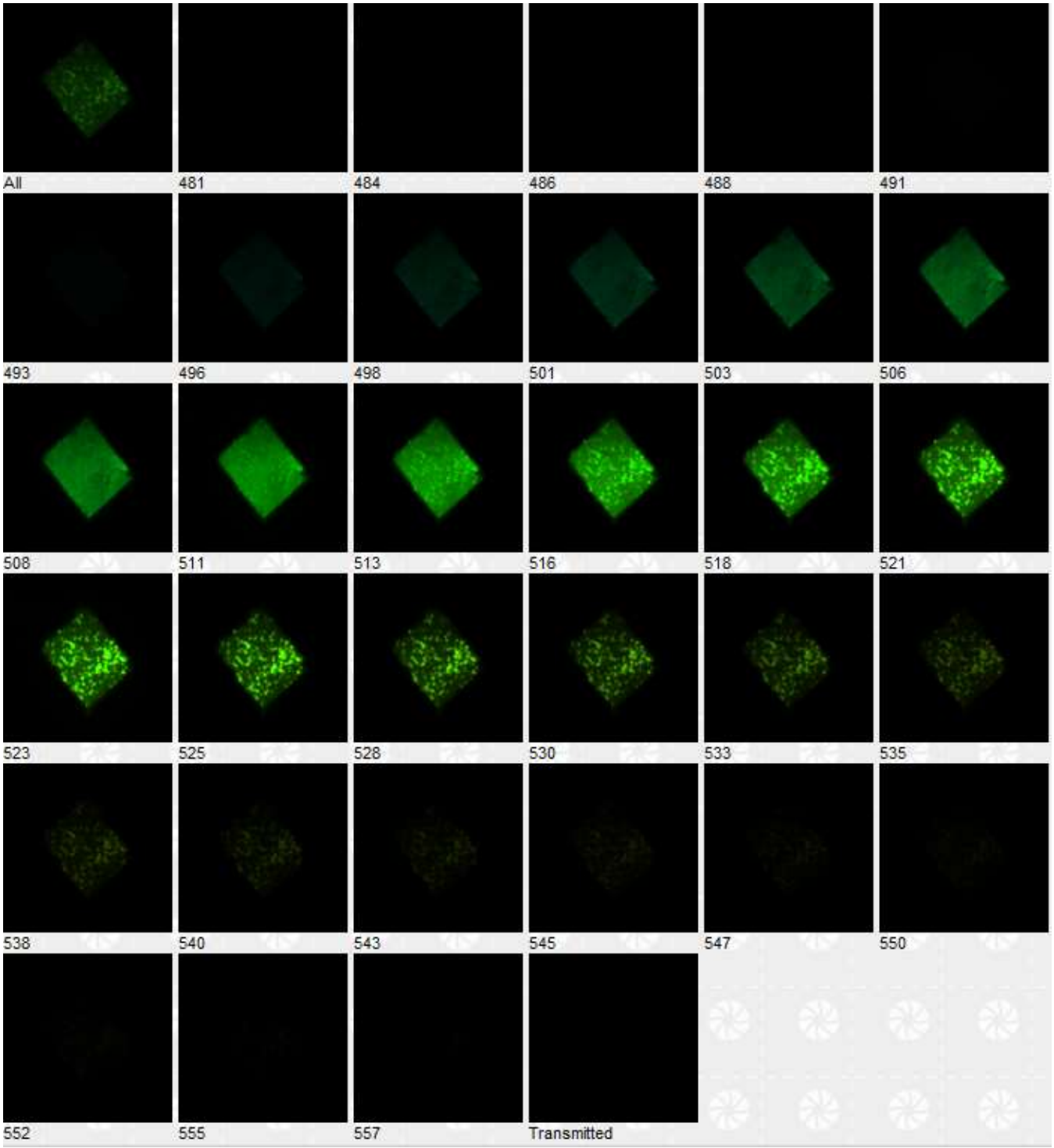

Figure S19. A grid of spectral channels for a single *z* slice 11/19, "-5.00μm" (see preceding figure). The number under each square indicates center wavelength of the channel in nm. Each square has dimensions of 15.55 μm x 15.55 μm.

The *z* slice 11/19 was chosen as a representative of the surface of the SL with impurities. The spatial distribution of the PL signal is interpreted in the following way: the PL signal in the range of ~496-508 nm is dominated by the NCs of the SL (no bright spots are visible), while PL in the range of ~516-545 nm is dominated by the impurities (bright spots are prominent).

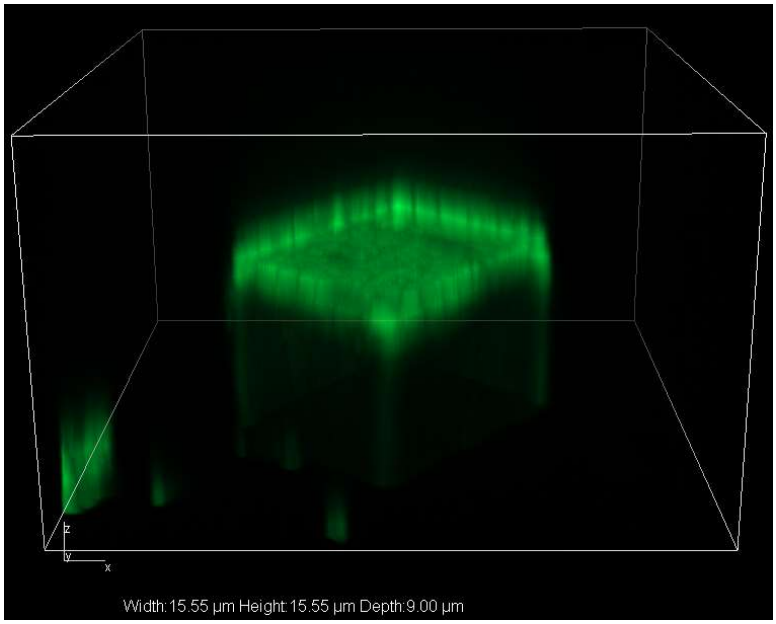

Figure S20. Spectrally filtered confocal PL volume view of the entire SL with impurities. The image is constructed by showing a PL signal coming from the ~496-508 nm spectral region.

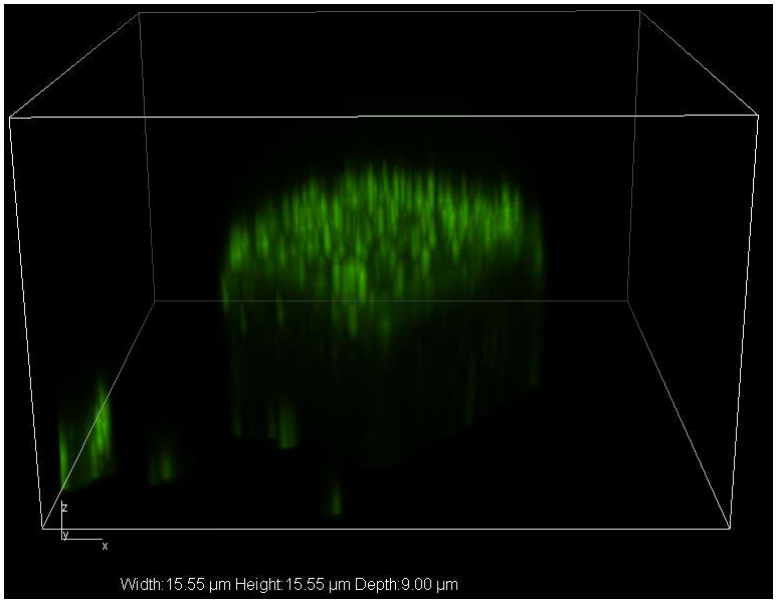

Figure S21. Spectrally filtered confocal PL volume view of the entire SL with impurities. The image is constructed by showing a PL signal coming from the ~516-545 nm spectral region.

The comparison between two spectrally filtered confocal PL volume views of the SL with impurities visualizes the spatial distribution of the emitters with a PL in different spectral regions: ~496-508 nm (Figure S20) and ~516-545 nm (Figure S21). In Figure S20, the flat rectangular surface of the SL is clearly visible, indicating that the PL signal is dominated by the NCs of the SL. In Figure S21, the PL signal is clearly dominated by the impurities (bright spots).

S10. Confocal PL microscopy *z* slices of a clean $CsPbBr_3$ NC SL

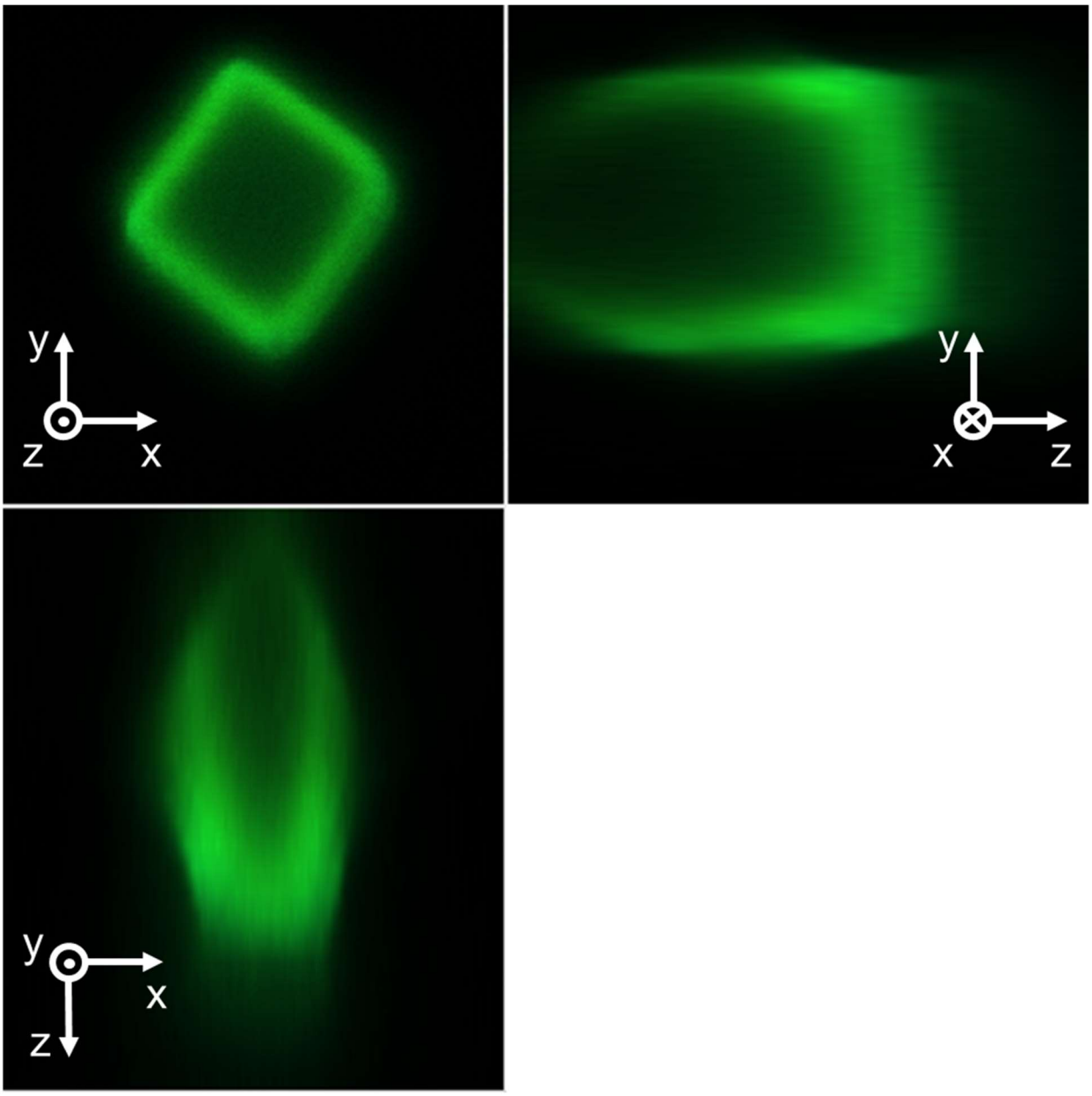

Figure S22. Confocal PL microscopy projections reconstructed from the *z* slices of the SL with a clean surface (further referred to as a "clean SL"). The impurities appear as bright spots. The projections are shown with all spectral channels on (spectral range of ~481-557 nm). *xy* plane projection (upper left image) has dimensions of 10.66 μm x 10.66 μm, *yz* and *xz* plane projections (upper right and lower left images, respectively) have dimensions of 10.66 μm along *y* and *x*-axes, and 12.00 μm along *z*-axis.

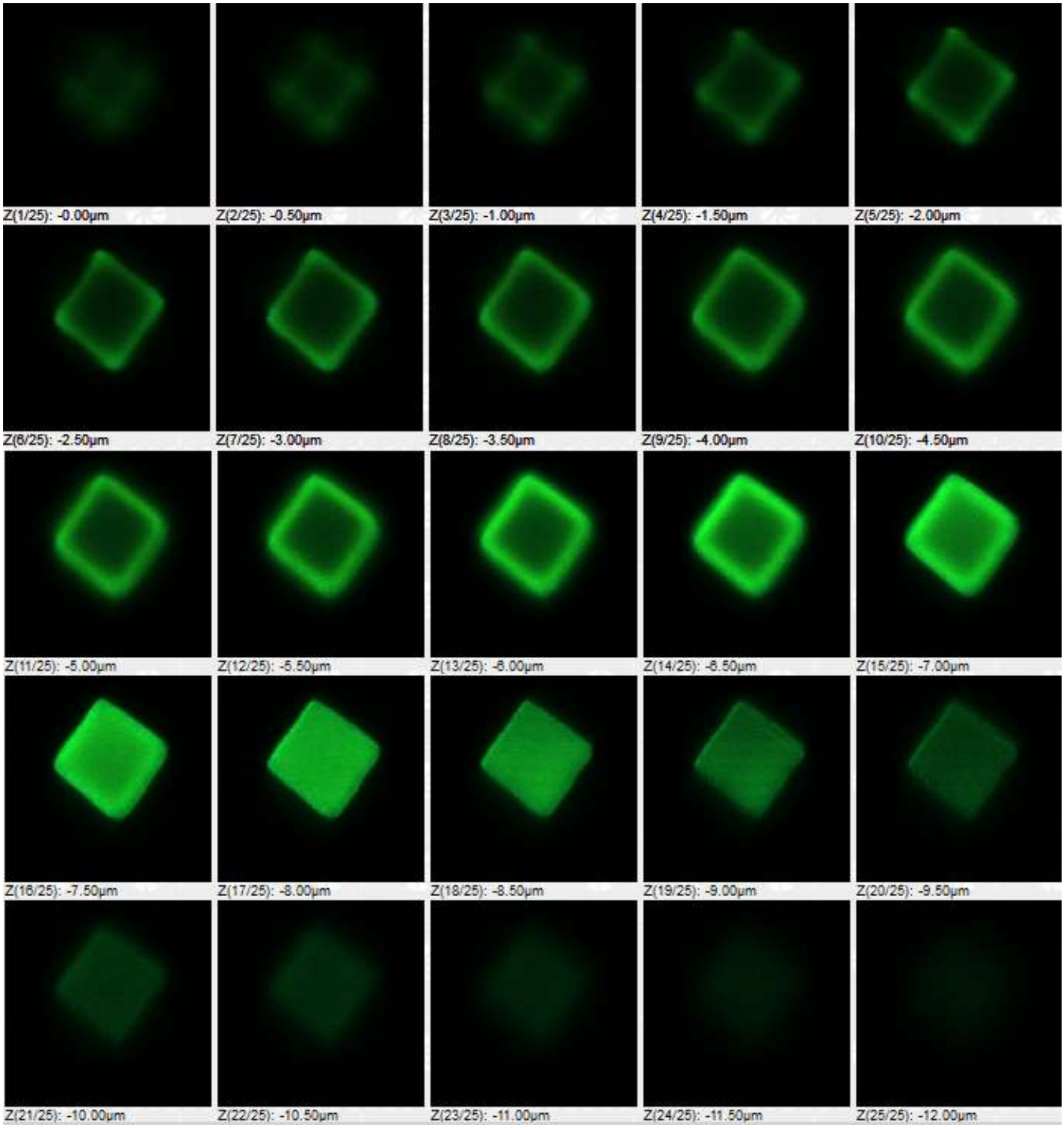

Figure S23. A grid of the z-slices showing the distribution of the PL signal from a clean SL as a function of the position of the focal plane. The total of 25 slices are shown, the slices are arranged from left to right in four rows. z step size is 0.5 µm, z range is from "-0.00µm" (bottom of the SL) to "-12.00 µm" (over the top of the SL). The image dimensions are 10.66 x 10.66 µm (512 x 512 pixels).

In contrast to the similar series captured for an SL with impurities, a clean SL shows a spatially uniform distribution of the PL signal along the *z* dimension.

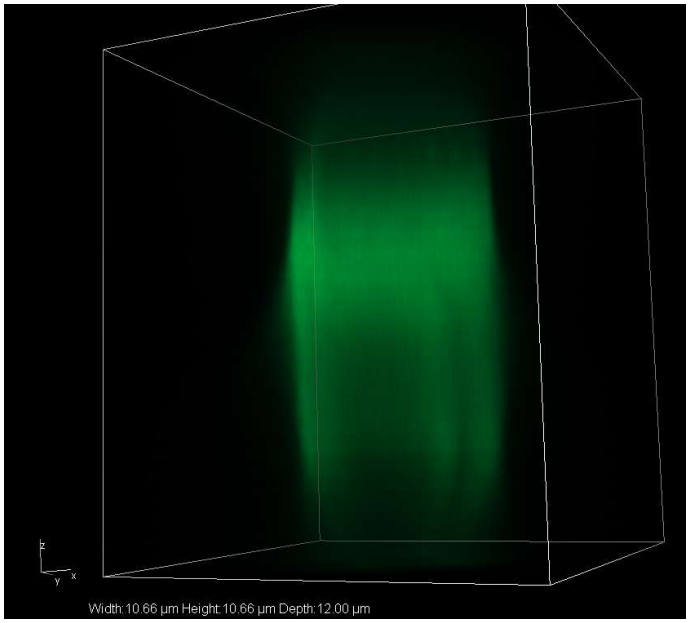

Figure S24. Spectrally filtered confocal PL volume view of an entire clean SL. The image is constructed by showing a PL signal coming from the ~496-508 nm spectral region.

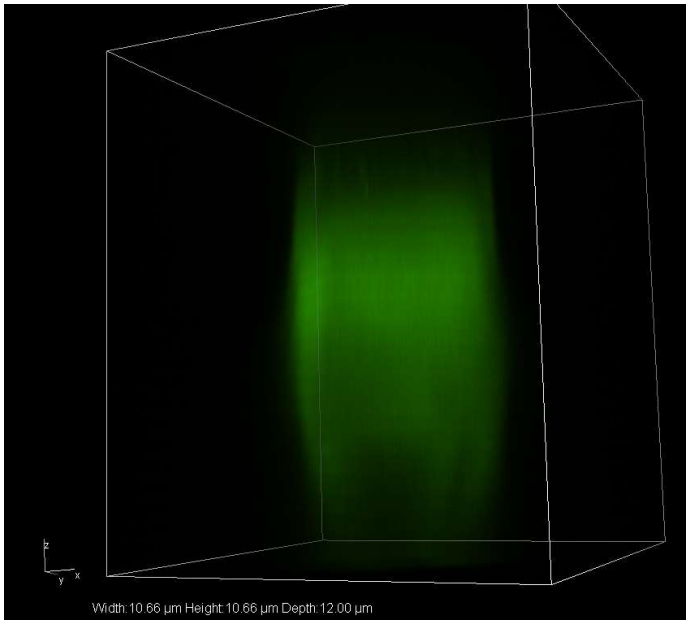

Figure S25. Spectrally filtered confocal PL volume view of an entire clean SL. The image is constructed by showing a PL signal coming from the ~516-545 nm spectral region.

Both spectrally filtered confocal PL volume views show a uniform emission originating from NCs in a clean SL.

S11. HRSEM analysis of the impurities on the surface of $CsPbBr_3$ NC SLs

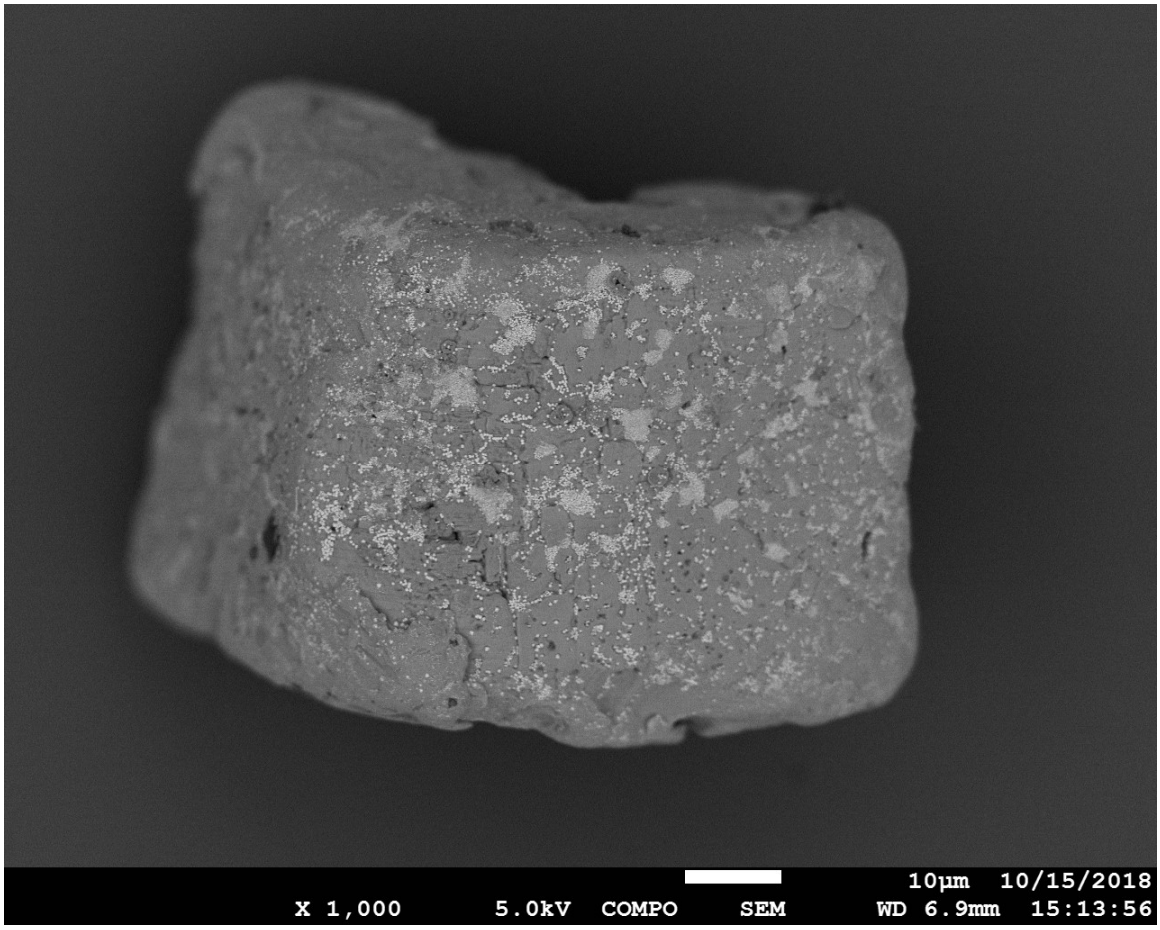

Figure S26. Low magnification HRSEM image of a large $CsPbBr_3$ NC SL with impurities on the surface (bright spots).

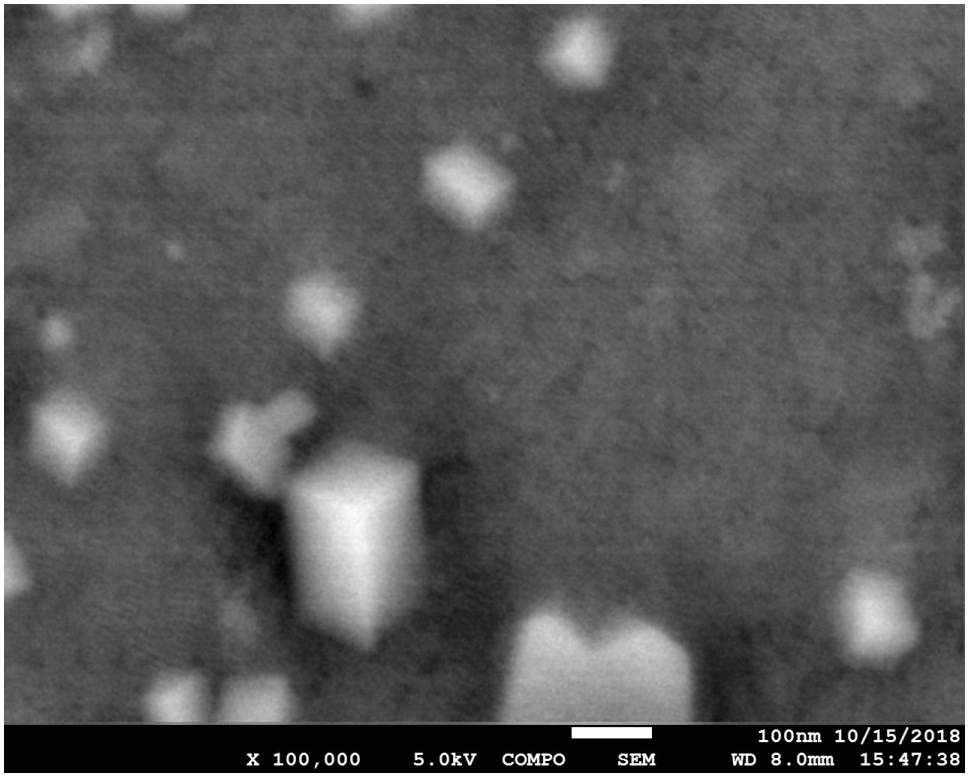

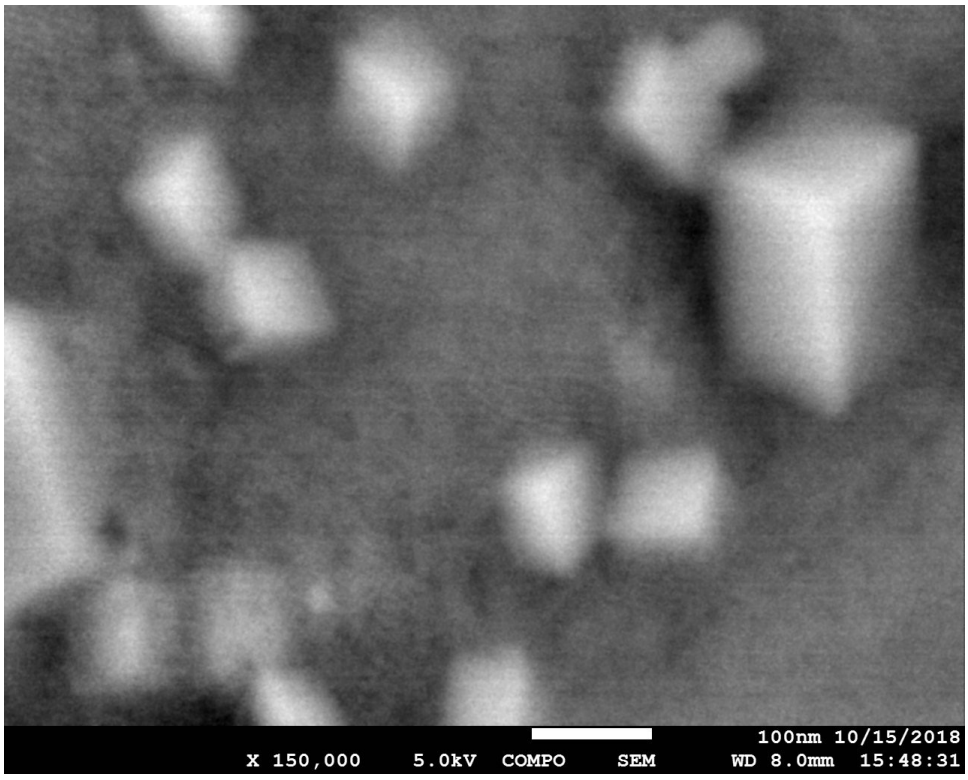

Figure S27. High magnification HRSEM images of the impurities on the surface of $CsPbBr_3$ NC SL. The images were FFT-filtered in ImageJ ver. 1.51j8 for clarity. [Procedure in the ImageJ: "Process" => "FFT" => "Bandpass Filter…"; filter parameters: filter large (small) structures down to ~200 (~3) nm, no stripes suppression, 5% tolerance of direction, "autoscale after filtering" box checked].

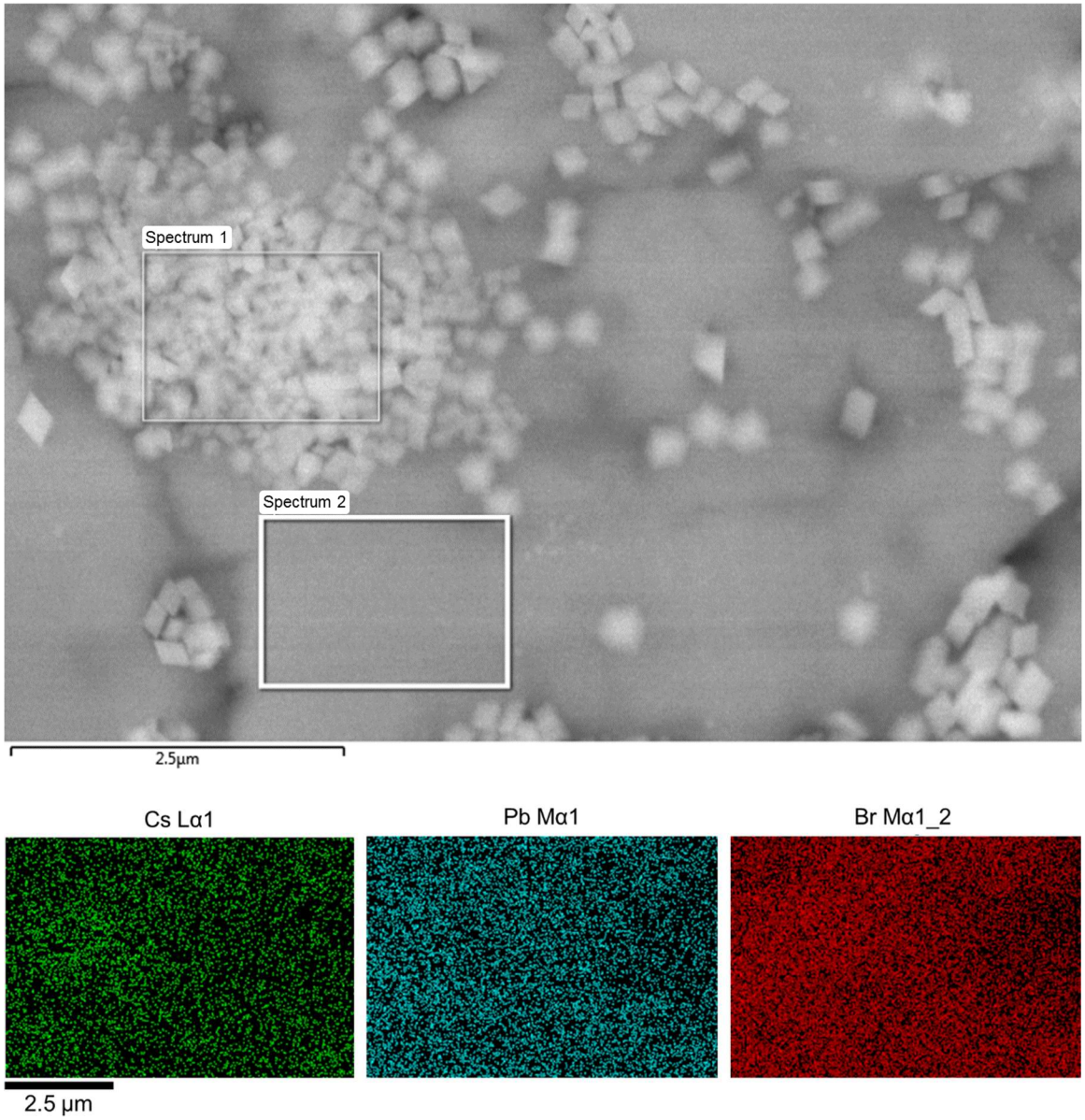

Figure S28. HRSEM image of the SL surface covered with impurities (bright rectangular objects) and elemental maps of the entire image showing the distribution of Cs, Pb, and Br elements. The boxes indicate regions from where elemental composition was acquired (Table S1).

Table S1. EDS analysis from two areas on the surface of $CsPbBr_3$ NC SL: the area covered with impurities (Spectrum 1), and an area without impurities (Spectrum 2).

Spectrum 1,	*Atomic %*		*Spectrum 2*	*Atomic %*
Cs	24.25		Cs	19.70
Pb	16.33		Pb	19.80
Br	59.43		Br	60.50
Total	*100.00*		*Total*	*100.00*

S12. Confocal PL microscopy of $CsPbBr_3$ NC SLs prepared by slow solvent evaporation

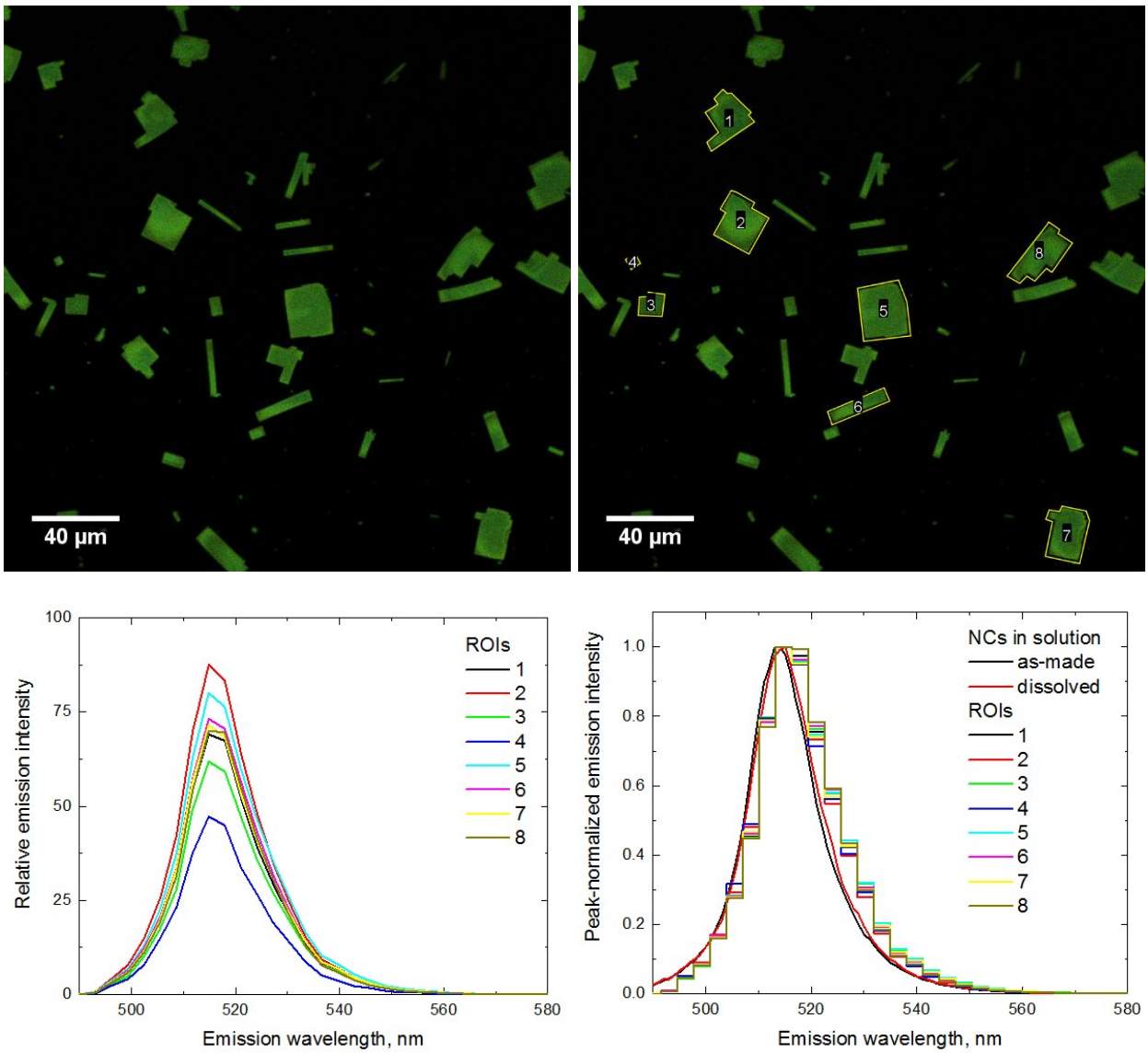

Figure S29. Confocal photoluminescence image (top left) of $CsPbBr_3$ NC SLs grown by slow solvent evaporation on top of the tilted Si wafer and their spectra. The top right image shows 8 regions of interest whose spectra are shown in the panels below. The bottom right image compares spectra from individual superlattices with emission spectra of NCs in solution recorded before self-assembly ("as-made") and dissolved superlattices ("dissolved"), the step plot is to indicate spectral resolution (3.1 nm). The spectra of NC solutions were recorded with 350 nm excitation.

S13. References

1. De Roo, J.; Ibáñez, M.; Geiregat, P.; Nedelcu, G.; Walravens, W.; Maes, J.; Martins, J. C.; Van Driessche, I.; Kovalenko, M. V.; Hens, Z., Highly Dynamic Ligand Binding and Light Absorption Coefficient of Cesium Lead Bromide Perovskite Nanocrystals. *ACS Nano* **2016,** 10, (2), 2071-2081.

2. Stoumpos, C. C.; Malliakas, C. D.; Peters, J. A.; Liu, Z.; Sebastian, M.; Im, J.; Chasapis, T. C.; Wibowo, A. C.; Chung, D. Y.; Freeman, A. J.; Wessels, B. W.; Kanatzidis, M. G., Crystal Growth of the Perovskite Semiconductor CsPbBr3: A New Material for High-Energy Radiation Detection. *Cryst. Growth Des.* **2013,** 13, (7), 2722-2727.

3. Bertolotti, F.; Protesescu, L.; Kovalenko, M. V.; Yakunin, S.; Cervellino, A.; Billinge, S. J. L.; Terban, M. W.; Pedersen, J. S.; Masciocchi, N.; Guagliardi, A., Coherent Nanotwins and Dynamic Disorder in Cesium Lead Halide Perovskite Nanocrystals. *ACS Nano* **2017,** 11, (4), 3819-3831.

4. Cottingham, P.; Brutchey, R. L., On the crystal structure of colloidally prepared CsPbBr3 quantum dots. *Chem. Commun.* **2016,** 52, (30), 5246-5249.

5. Lakowicz, J. R., *Principles of Fluorescence Spectroscopy*. 3rd ed ed.; 2009.

6. Schneider, C. A.; Rasband, W. S.; Eliceiri, K. W., NIH Image to ImageJ: 25 years of image analysis. *Nat. Methods* **2012,** 9, 671.

7. Schindelin, J.; Arganda-Carreras, I.; Frise, E.; Kaynig, V.; Longair, M.; Pietzsch, T.; Preibisch, S.; Rueden, C.; Saalfeld, S.; Schmid, B.; Tinevez, J.-Y.; White, D. J.; Hartenstein, V.; Eliceiri, K.; Tomancak, P.; Cardona, A., Fiji: an open-source platform for biological-image analysis. *Nat. Methods* **2012,** 9, 676.

8. http://imagej.net/ImageJ.

9. Park, S. D.; Baranov, D.; Ryu, J.; Cho, B.; Halder, A.; Seifert, S.; Vajda, S.; Jonas, D. M., Bandgap Inhomogeneity of a PbSe Quantum Dot Ensemble from Two-Dimensional Spectroscopy and Comparison to Size Inhomogeneity from Electron Microscopy. *Nano Lett.* **2017,** 17, (2), 762-771.

10. Segets, D.; Lucas, J. M.; Klupp Taylor, R. N.; Scheele, M.; Zheng, H.; Alivisatos, A. P.; Peukert, W., Determination of the Quantum Dot Band Gap Dependence on Particle Size from Optical Absorbance and Transmission Electron Microscopy Measurements. *ACS Nano* **2012,** 6, (10), 9021-9032.